ments. The cells were subsequently stained with Hoechst 33342 for 10 min and subjected to confocal fluorescence microscopy.

The confocal microscopic study of the RAW264.7 cells treated with compound **1** indicated that **1** was localized to the cell membrane as expected (Fig. 2), due to the presence of its alkyl chain. The TEMPO moiety was assumed to be close to the surface in the lipid bilayer because the signal shape was not broad, as compared with the signal of TEMPOL in solution (Supporting information). This probe is considered to be able to penetrate into the lipid bilayer for its adequate lipid solubility. Compounds **1** and **2** are assumed to be distributed at the both leaflets of the cell membrane. Thus, the probe can measure the oxidative stress at the cell membrane (Scheme 1 and Scheme 2).

There are no differences in localization and sensitivity between compounds **1** and **2** in the observation by confocal fluorescence microscopy. Compound **1** was used for ESR analysis because it was more stable than compound **2** in solution. The ESR signal of **1** was measured in RAW264.7 cells to evaluate oxidative stress in the cell

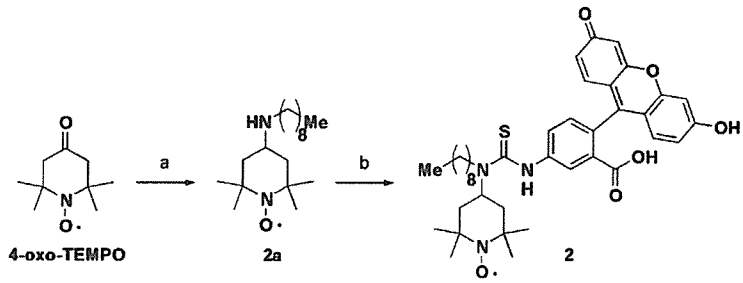

Scheme 2. Synthesis of compound **2**. Reagents and conditions: (a) *n*-nonylamine, THF, then $NaBH(OAc)_3$, 84%; (b) FITC, THF, 41%.

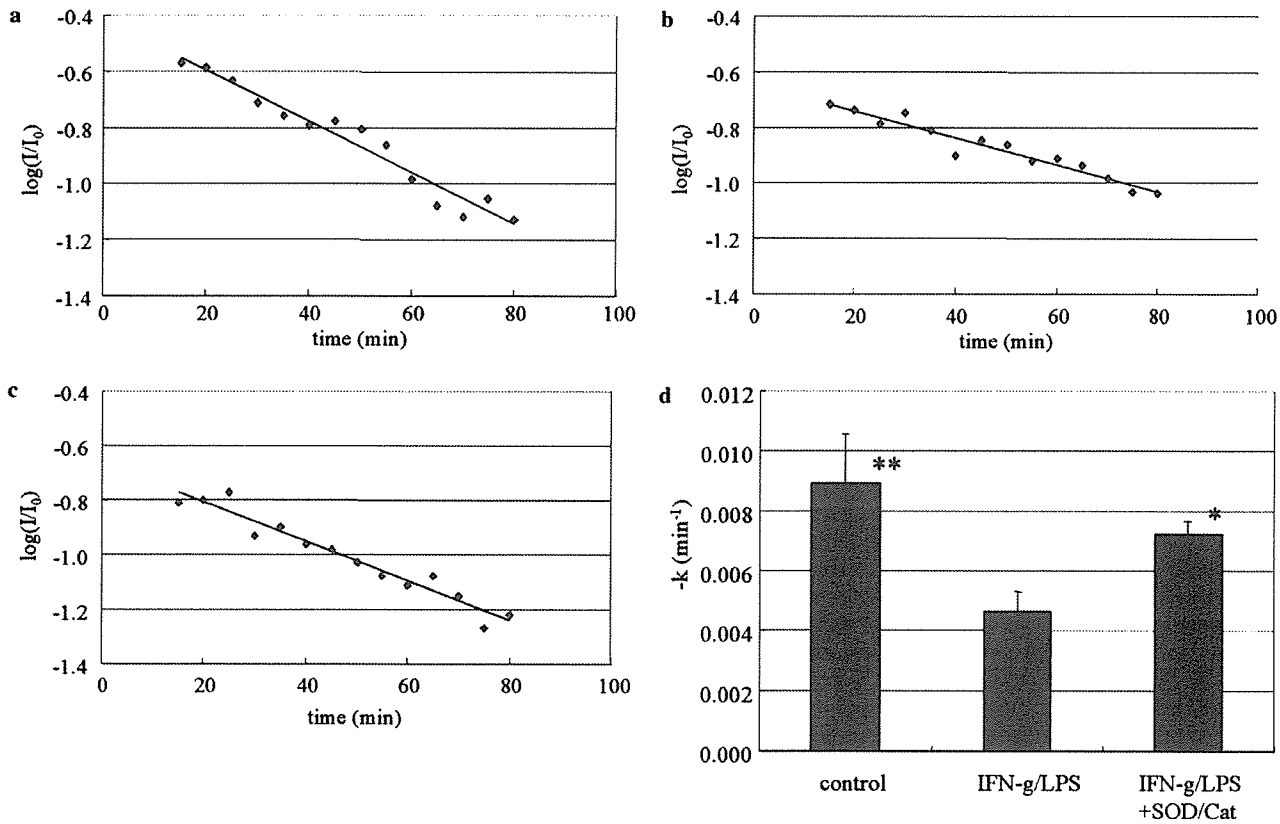

Figure 3. The time course of the relative signal intensity measured at 5-min intervals, (a) control cells, (b) LPS/IFN-γ-treated cells, and (c) LPS/IFN-γ-treated cells in the presence of SOD and catalase. *I*, compound 1 peak area; I_0, Mn^{2+} external standard peak area. (d) Signal decay rate of **1** in RAW264.7 cells. The signal decay rates of **1** with RAW264.7 cells were calculated from ESR signal intensities of **1** in RAW264.7 cells treated with vehicle, or with LPS/IFN-γ in the presence or absence of SOD/catalase. Values are presented as means ± SD of 3 or 4 experiments. ANOVA and Bonferroni-type multiple *t*-test indicated significant differences between LPS/IFN-γ and the control ($^{**}P < 0.01$), and LPS/IFN-γ + SOD/catalase ($^{*}P < 0.05$).

membrane. In the control cells, the signal intensity of **1** was gradually decreased at $0.0091 \pm 0.002\ min^{-1}$ under our conditions. The upregulation of oxidative stress was evaluated after endotoxic stimulation. ESR spectra of **1** were measured in RAW264.7 cells treated with 500 ng/mL LPS and 150 U/mL IFN-γ for 5 h. The rate of signal decay observed in cells treated with LPS/IFN-γ was decreased to $0.0049 \pm 0.0007\ min^{-1}$. The decreased rate as a result of the LPS/IFN-γ treatment was restored to $0.0072 \pm 0.0004\ min^{-1}$ in the presence of 100 U/mL SOD and 10 U/mL catalase during measurement (Fig. 3d). In the absence of the RAW264.7 cells, the signal failed to decay (data not shown).

Since cells generally exist in a reductive environment, compound **1** was found to be gradually reduced to the non-radical species in the presence of the control cells. Treatment with LPS/IFN-γ activated the cells and increased the production of reactive oxygen and nitrogen species (ROS/RNS). LPS/IFN-γ treatment also decreased the decay rate of nitroxyl radical. The decrease in this rate was recovered in the presence of 100 U/mL SOD and 10 U/mL catalase. Although ROS were still upregulated by LPS/IFN-γ treatment, they were considered to be at least partially scavenged by SOD and catalase. The probe was reduced under any conditions in our experiment, and the decay rate was considered to reflect the cellular local reducing ability for the probe, which would correlate with the oxidative stress in the cell membrane. Thus, the decay rate of **1** was not assumed to reflect specific ROS production, but the local oxidant upregulation, although the production of superoxide was upregulated under this experimental condition, and superoxide, hydrogen peroxide, and hydroxyl radical were considered to play an important role in this result. It was suggested that the cell membrane was exposed to an oxidative environment due to the increase in ROS by LPS/IFN-γ-pretreatment. Although SOD and catalase were thought not to be distributed inside the cells, they were able to get close to the cell membrane, where compound **1** was localized. These two enzymes may contribute to the scavenging of ROS around the cell membrane, and this is consistent with the fact that ESR signal decay rate was restored under these conditions. The change in this rate was assumed to be due to either a decrease in the cellular reductants by ROS upregulation or an increase in the oxidation of hydroxylamine, a reduced form of **1**.[9] The TEMPO moiety can be oxidized to the ESR-silent oxonium cation form by superoxide.[10] However, this cation was found to be rapidly reduced back to TEMPO by the superoxide itself.[10] Compound **1** was considered to be repeatedly oxidized and reduced in the cell membrane. The direct oxidation of TEMPO itself by superoxide probably does not affect the signal decay rate under the condition used for these measurements.

In conclusion, although there remain some detailed characteristics to be clarified, compound **1** was found to be a useful probe for evaluating oxidative stress at the cell membrane.

Supplementary data

Supplementary data associated with this article can be found, in the online version, at doi:10.1016/j.bmcl.2006.11.040.

References and notes

1. (a) Irani, K.; Goldschmidt-Clermont, P. J. *Biochem. Pharmacol.* **1998**, *55*, 1339; (b) Irani, K.; Xia, Y.; Zweier, J. L.; Sollott, S. J.; Der, C. J.; Fearon, E. R.; Sundaresan, M.; Finkel, T.; Goldschmidt-Clermont, P. J. *Science* **1997**, *275*, 1649.
2. Darley-Usmar, V.; Halliwell, B. *Pharm. Res* **1996**, *13*, 649.
3. (a) Ballinger, S. W. *Free Radic. Biol. Med.* **2005**, *38*, 1278; (b) Molavi, B.; Mehta, J. L. *Curr. Opin. Cardiol.* **2004**, *19*, 488.
4. (a) Love, S. *Brain Pathol.* **1999**, *9*, 119; (b) Sweeney, M. I.; Yager, J. Y.; Walz, W.; Juurlink, B. H. *Can. J. Physiol. Pharmacol.* **1995**, *75*, 1525.
5. (a) Wipf, P.; Xiao, J.; Jiang, J.; Belikova, NA.; Tyurin, V. A.; Fink, M. P.; Kagan, V. E. *J. Am. Chem. Soc.* **2005**, *127*, 12460; (b) Okamoto, A.; Inasaki, T.; Saito, I. *Bioorg. Med. Chem. Lett* **2004**, *14*, 3415; (c) Freedman, J. E.; Keaney, J. F., Jr. *Methods Enzymol.* **1999**, *301*, 61.
6. Nakagawa, H.; Moritake, T.; Tsuboi, K.; Ikota, N.; Ozawa, T. *FEBS Lett.* **2000**, *471*, 187.
7. (a) May, J. M.; Qu, Z. C.; Juliao, S.; Cobb, C. E. *Free Radic. Res.* **2005**, *39*, 195; (b) Samuni, A.; Goldstein, S.; Russo, A.; Mitchell, J. B.; Krishna, M. C.; Neta, P. *J. Am. Chem. Soc.* **2002**, *124*, 8719; (c) Iannone, A.; Bini, A.; Swartz, HM.; Tomasi, A.; Vannini, V. *Biochem. Pharmacol.* **1989**, *38*, 2581.
8. Cuzzocrea, S.; McDonald, M. C.; Mazzon, E.; Dugo, L.; Lepore, V.; Fonti, M. T.; Ciccolo, A.; Terranova, M. L.; Caputi, A. P.; Thiemerann, C. *Eur. J. Pharmacol.* **2000**, *406*, 127.
9. Zigler, J. S., Jr.; Qin, C.; Kamiya, T.; Krishna, MC.; Cheng, Q.; Tumminia, S.; Russell, P. *Free Radic. Biol. Med.* **2003**, *35*, 1194.
10. Krishna, MC.; Russo, A.; Mitchell, JB.; Goldstein, S.; Dafni, H.; Samuni, A. *J. Biol. Chem.* **1996**, *271*, 26026.

Available online at www.sciencedirect.com

ScienceDirect

Bioorganic & Medicinal Chemistry Letters

ELSEVIER

Bioorganic & Medicinal Chemistry Letters 17 (2007) 1558–1561

Identification of a potent and stable antiproliferative agent by the prodrug formation of a thiolate histone deacetylase inhibitor

Takayoshi Suzuki,[a,*] Shinya Hisakawa,[a] Yukihiro Itoh,[a] Sakiko Maruyama,[b] Mineko Kurotaki,[b] Hidehiko Nakagawa[a] and Naoki Miyata[a,*]

[a]*Graduate School of Pharmaceutical Sciences, Nagoya City University, 3-1 Tanabe-dori, Mizuho-ku, Nagoya, Aichi 467-8603, Japan*
[b]*Evaluation Group, Drug Research Department, R&D Division, Pharmaceuticals Group, Nippon Kayaku Co., Ltd, 31-12, Shimo 3-chome, Kita-ku, Tokyo 115-8588, Japan*

Received 29 November 2006; revised 22 December 2006; accepted 29 December 2006
Available online 13 January 2007

Abstract—To identify prodrugs of a thiolate histone deacetylase inhibitor NCH-31 that show potent antiproliferative activity and are stable in human plasma, we synthesized several candidate prodrugs of NCH-31. Among these compounds, *S*-2-methyl-3-phenylpropanoyl compound **2** showed more potent antiproliferative activity and higher stability in human plasma than *S*-isobutyryl compound NCH-51.

The dynamic homeostasis of the nuclear acetylation of histones is regulated by the opposing activity of the enzymes histone acetyl transferases and histone deacetylases (HDACs).[1,2] Deacetylation of histone lysine residues is associated with a condensed chromatin structure resulting in transcriptional repression, whereas acetylation of histones is associated with a more open chromatin configuration and activation of transcription.[3] Aberrant activation of HDACs results in the transcriptional repression of oncoprotein and is linked to the malignant phenotypes of tumors.[4,5] Inhibition of HDACs causes histone hyperacetylation which leads to the disruption of the chromatin structure and the transcriptional activation of genes associated with cancer.[3,6] In addition, it has recently been reported that inhibition of an HDAC exerts antitumor effects through the non-transcriptional pathway in addition to the intervention of transcriptional regulation.[7,8] Indeed, HDAC inhibitors such as trichostatin A (TSA) and suberoylanilide hydroxamic acid (SAHA) (Fig. 1) have potent anticancer effects in vitro and in vivo.[9,10]

In the course of our study of HDAC inhibitors, we found that a series of thiol-based analogues, including NCH-31 (Fig. 2), are potent HDAC inhibitors.[11] Thiols are thought to inhibit HDACs by coordinating the zinc ion in the active site which is required for deacetylation of the acetylated lysine substrate. Further, the *S*-isobutyryl prodrug NCH-51 (Fig. 2), which is thought to be hydrolyzed to free thiol within cells, showed antiproliferative activity against cancer cells,[12] however, NCH-51 has stability problems. NCH-51 was vulnerable to human plasma metabolism at the remaining rate of approximately 50% after 24 h of incubation. We therefore decided to search for prodrugs that are more stable in human plasma and exert more potent antiproliferative activity than NCH-51.

Since prodrugs with a less hindered acyl group tended to exhibit less potent antiproliferative activity,[12] we designed *S*-acyl prodrugs **1**–**4** which bear an acyl group more bulky than NCH-51. Four candidate prodrugs of NCH-31 were synthesized as shown in Scheme 1. The sulfhydryl group of NCH-31 was acylated with the corresponding carboxylic acid to give the desired compounds **1**–**4**.

The compounds synthesized in this study were initially tested in antiproliferative activity assays using human lung cancer NCI-H460 cells and human breast cancer MDA-MB-231 cells (Table 1).[13] Although *S*-2-methoxy-2-phenylacetyl compound **3** and 3-phenyl-2-(phenylmethyl)propanoyl compound **4** were less active than thiol NCH-31 and its *S*-isobutyryl prodrug NCH-51,

Keywords: Histone deacetylase inhibitor; Antiproliferative agent; Prodrug.
* Corresponding authors. Tel./fax: +81 52 836 3407 (N. M.); e-mail addresses: suzuki@phar.nagoya-cu.ac.jp; miyata-n@phar.nagoya-cu.ac.jp

0960-894X/$ - see front matter © 2007 Elsevier Ltd. All rights reserved.
doi:10.1016/j.bmcl.2006.12.117

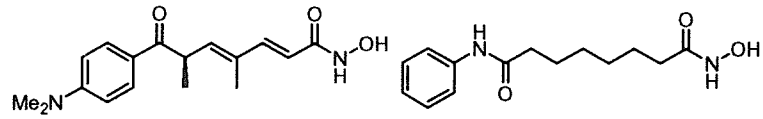

TSA SAHA

Figure 1. Structures of TSA and SAHA.

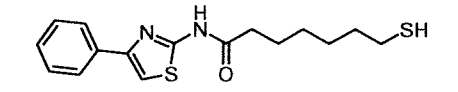

NCH-31

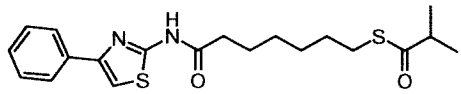

NCH-51

Figure 2. Structures of NCH-31 and NCH-51.

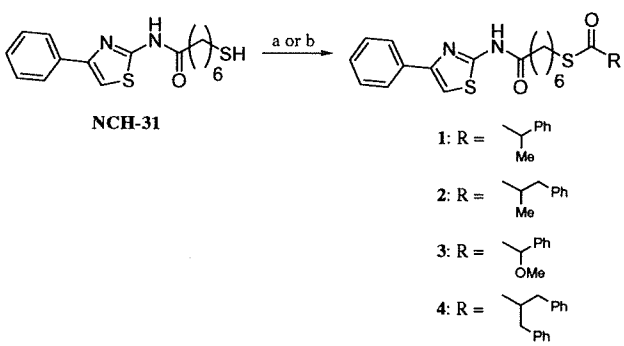

Scheme 1. Reagents and conditions: (a) RCOCl (for 1 and 4), DMAP, pyridine, 0 °C to rt, 41% for 1, 54% for 4; (b) RCOOH (for 2 and 3), EDCI, DMAP, DMF, rt, 63% for 2, 23% for 3.

S-2-phenylpropanoyl compound **1** showed similar activity against NCI-H460 cells and *S*-2-methyl-3-phenylpropanoyl compound **2** also displayed similar activity against both NCI-H460 cells and MDA-MB-231 cells when compared with NCH-51. Furthermore, we examined proliferation inhibition by NCH-51, compounds **1** and **2**, against eight solid cancer cell lines. As can be seen from Table 2, compound **2** showed potent proliferation inhibition against various cancer cells representing a 2-fold improvement over NCH-51 (average EC_{50} of **2** 2.4 μM, NCH-51 4.9 μM).

To investigate the difference in activity between (*R*)-**2** and (*S*)-**2**, optically active (*R*)-**2** and (*S*)-**2** were prepared from (*S*)-4,5,5-trimethyloxazolidin-2-one **5**[14] as outlined in Scheme 2. The chiral auxiliary **5** was converted to compounds **6** and **7** by *N*-propionylation and *N*-3-phenylpropionylation, respectively. Stereoselective enolate benzylation of **6** and methylation of **7**, and the subsequent hydrolysis of **8** and **9** gave optically active 2-methyl-3-phenylpropanoic acids (*R*)-**10** and (*S*)-**10**, respectively. The condensation of carboxylic acids

Table 1. Proliferation inhibition data on NCI-H460 cells and MDA-MB-231 cells for NCH-31, NCH-51, and compounds **1–4**[a]

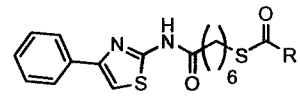

Compound	R	EC_{50} (μM)	
		NCI-H460	MDA-MB-231
NCH-31	–H	7.6	>20
NCH-51		2.1	4.4
1		3.2	>20
2	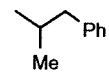	1.5	1.9
3		11	>20
4	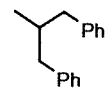	>20	>20

[a] Values are means of at least two experiments.

(*R*)-**10** and (*S*)-**10** with NCH-31 in the presence of EDCI and DMAP afforded optically active (*R*)-**2** and (*S*)-**2**, respectively. The enantiomeric excess of both (*R*)-**2** and (*S*)-**2** was determined to be 90% by chiral column chromatography.[15]

We examined the antiproliferative activity of (*R*)-**2** and (*S*)-**2** against four cancer cell lines, and there was not much difference between the activities of the two stereoisomers (Table 3).

Next, we investigated the in vitro HDAC inhibitory activity of compound **2** (Table 4).[16] Although NCH-31 exhibited potent inhibitory activity against HDAC1 (IC_{50} = 0.048 μM), the *S*-2-methyl-3-phenylpropanoyl prodrug **2** did not inhibit HDAC1 at a concentration of 100 μM.

Compound **2** was evaluated for the accumulation of acetylated histone H4 using Western blot analysis (Fig. 3).[17] Treatment of HCT116 cells with compound **2** produced an increase in the accumulation of acetylated histone H4, which indicated that the antiproliferative activity of compound **2** significantly correlates with the inhibition of HDACs. Since *S*-2-methyl-3-phenylpropanoyl prodrug **2** was totally inactive in an enzyme assay

Table 2. Proliferation inhibition data on eight human solid cancer cell lines for NCH-51, compounds **1** and **2**[a]

Cell		NCH-51, EC_{50} (μM)	**1**, EC_{50} (μM)	**2**, EC_{50} (μM)
T-47D	Breast cancer	8.3	>100	4.3
MDA-MB-231	Breast cancer	4.4	27	1.9
NCI-H460	Lung cancer	2.1	3.2	1.5
A498	Renal cancer	6.8	26	2.6
PC-3	Prostate cancer	9.5	37	3.2
DLD-1	Colon cancer	2.3	86	1.8
HCT116	Colon cancer	1.3	23	1.2
MALME-3M	Melanoma	4.3	33	3.0
Mean		4.9	42	2.4

[a] Values are means of at least two experiments.

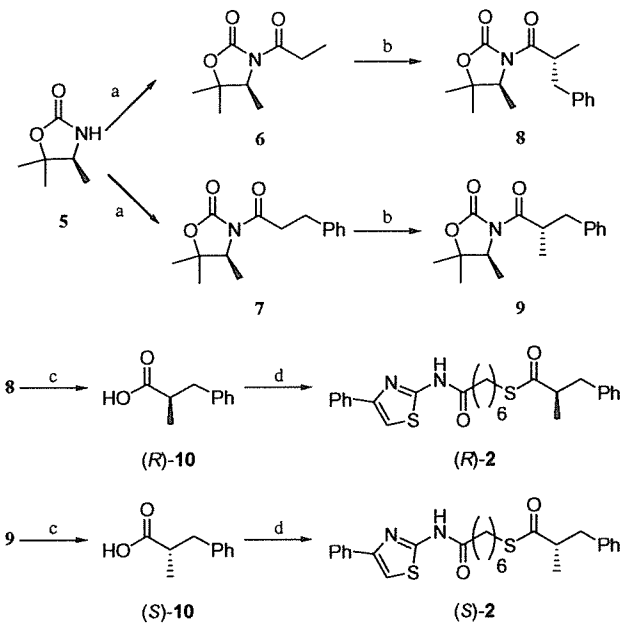

Scheme 2. Reagents and conditions: (a) i—*n*-BuLi, THF, −78 °C; ii—propionyl chloride (for **6**) or 3-phenylpropionyl chloride (for **7**), THF, −78 °C, 71% for **6**, 83% for **7**; (b) i—LDA, THF, −78 °C; ii—BnBr (for **8**) or MeI (for **9**), THF, −78 °C to rt, 71% for **8**, 63% for **9**; (c) LiOH·H_2O, THF, H_2O, 0 °C to rt, 77% for (*R*)-**10**, 78% for (*S*)-**10**; (d) NCH-31, EDCI, DMAP, CH_2Cl_2, rt, 57% for (*R*)-**2**, 52% for (*S*)-**2**.

Table 3. Proliferation inhibition data on four human solid cancer cell lines for (*R*)-**2** and (*S*)-**2**[a]

Cell		(*R*)-**2**, EC_{50} (μM)	(*S*)-**2** EC_{50} (μM)
MDA-MB-231	Breast cancer	3.1	4.0
NCI-H460	Lung cancer	3.2	3.0
PC-3	Prostate cancer	9.9	4.4
HCT116	Colon cancer	0.75	0.62

[a] Values are means of at least two experiments.

(Table 4), it could possibly permeate the cell membrane and be converted to active free thiol NCH-31 by enzymatic hydrolysis within the cell.

Finally, we assessed the stability of compound **2** in human plasma (Table 5).[18] Interestingly, compound **2** was found to be tolerant to human plasma metabolism. Nearly 100% of the intact compound was observed even after 24-h incubation in human plasma.

Table 4. HDAC1 inhibition data for TSA, NCH-31, and compound **2**[a]

Compound	IC_{50} (μM)
TSA	0.026
NCH-31	0.048
2	>100[b]

[a] Values are means of at least three experiments.
[b] 19% inhibition at 100 μM.

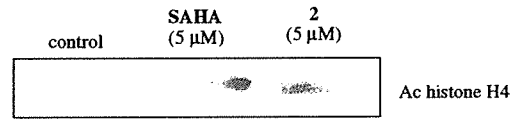

Figure 3. Western blot analysis of histone hyperacetylation in HCAT116 cells produced by compound **2** and by reference compound SAHA.

In summary, to identify potent prodrugs of a thiolate HDAC inhibitor, NCH-31, that are more stable in human plasma than NCH-51, we designed and prepared several candidate prodrugs of NCH-31. Among these compounds, *S*-2-methyl-3-phenylpropanoyl compound **2** showed more potent antiproliferative activity than *S*-isobutyryl compound NCH-51. Compound **2** also displayed high stability in human plasma. Further study pertaining to compound **2** is underway to investigate the therapeutic efficacy against human cancers.

Table 5. Stability of NCH-51 and compound **2** in human plasma[a]

Compound	%*R*[b]				
	0h	2h	4h	8h	24h
NCH-51	100	86	71	63	49
2	100	100	99	99	100

[a] Values are means of at least three experiments.
[b] The percentage of the parent compound remaining (%*R*) was measured after 2, 4, 8, and 24 h incubation at 37 °C.

Acknowledgments

This research was partly supported by Grants-in Aid for Young Scientists (B) from the Ministry of Education, Science, Culture, Sports, Science and Technology, Japan, Grants-in Aid for Research in Nagoya City University, and grants from the Japan Securities Scholarship Foundation, the Tokyo Biochemical Research Foundation, Takeda Science Foundation, and the TERUMO Lifescience Foundation. We thank the Screening Committee of New Anticancer Agents, supported by a Grant-in-Aid for Scientific Research on Priority Area 'Cancer' from the Ministry of Education, Culture, Sports, Science and Technology of Japan for HDAC1 inhibition assay results.

References and notes

1. Suzuki, T.; Miyata, N. *Curr. Med. Chem.* **2006**, *13*, 935.
2. Biel, M.; Wascholowski, V.; Giannis, A. *Angew. Chem. Int. Ed.* **2005**, *44*, 3186.
3. Taunton, J.; Hassig, C. A.; Schreiber, S. L. *Science* **1996**, *272*, 408.
4. Fraga, M. F.; Ballestar, E.; Villar-Garea, A.; Boix-Chornet, M.; Espada, J.; Schotta, G.; Bonaldi, T.; Haydon, C.; Ropero, S.; Petrie, K.; Iyer, N. G.; Perez-Rosado, A.; Calvo, E.; Lopez, J. A.; Cano, A.; Calasanz, M. J.; Colomer, D.; Piris, M. A.; Ahn, N.; Imhof, A.; Caldas, C.; Jenuwein, T.; Esteller, M. *Nat. Genet.* **2005**, *37*, 391.
5. Seligson, D. B.; Horvath, S.; Shi, T.; Yu, H.; Tze, S.; Grunstein, M.; Kurdistani, S. K. *Nature* **2005**, *435*, 1262.
6. Sambucetti, L. C.; Fischer, D. D.; Zabludoff, S.; Kwon, P. O.; Chamberlin, H.; Trogani, N.; Xu, H.; Cohen, D. *J. Biol. Chem.* **1999**, *274*, 34940.
7. Bali, P.; Pranpat, M.; Bradner, J.; Balasis, M.; Fiskus, W.; Guo, F.; Rocha, K.; Kumaraswamy, S.; Boyapalle, S.; Atadja, P.; Seto, E.; Bhalla, K. *J. Biol. Chem.* **2005**, *280*, 26729.
8. Hideshima, T.; Bradner, J. E.; Wong, J.; Chauhan, D.; Richardson, P.; Schreiber, S. L.; Anderson, K. C. *Proc. Natl. Acad. Sci. U.S.A.* **2005**, *102*, 8567.
9. Yoshida, M.; Horinouchi, S.; Beppu, T. *BioEssays* **1995**, *17*, 423.
10. Richon, V. M.; Emiliani, S.; Verdin, E.; Webb, Y.; Breslow, R.; Rifkind, R. A.; Marks, P. A. *Proc. Natl. Acad. Sci. U.S.A.* **1998**, *95*, 3003.
11. Suzuki, T.; Kouketsu, A.; Matsuura, A.; Kohara, A.; Ninomiya, S.; Kohda, K.; Miyata, N. *Bioorg. Med. Chem. Lett.* **2004**, *14*, 3313.
12. Suzuki, T.; Nagano, Y.; Kouketsu, A.; Matsuura, A.; Maruyama, S.; Kurotaki, M.; Nakagawa, H.; Miyata, N. *J. Med. Chem.* **2005**, *48*, 1019.
13. The antiproliferative activity assay was performed as follows. Cancer cells were plated in 96-well plates at initial density of 1500 cells/well and incubated at 37 °C. After 24 h, cells were exposed to test compounds at various concentrations in 10% FBS-supplemented RPMI-1640 medium at 37 °C in 5% CO_2 for 48 h. The medium was removed and replaced with 200 μL of 0.5 mg/mL of methylene blue in RPMI-1640 medium, and cells were incubated at room temperature for 30 min. Supernatants were removed from the wells, and methylene blue dye was dissolved in 100 μL/well of 3% aqueous HCl. Absorbance was determined on a microplate reader (Bio-Rad) at 660 nm.
14. Davies, S. G.; Sanganee, H. J. *Tetrahedron: Asymmetry* **1995**, *6*, 671.
15. Analytical conditions of chiral column chromatography; column: CHIRALCEL OA (Daicel Chemical Industries), eluent: *n*-hexane/isopropanol = 19:1, flow rate: 1 mL/min; retention time: 27.4 min ((*R*)-**2**), 29.3 min ((*S*)-**2**).
16. The inhibitory activities of test compounds against partially purified HDAC1 were assayed according to a method reported in the literature: Furumai, R.; Komatsu, Y.; Nishino, N.; Khochbin, S.; Yoshida, M.; Horinouchi, S. *Proc. Natl. Acad. Sci. U.S.A.* **2001**, *98*, 87.
17. Western blot analysis was performed as follows. HCT-116 cells (5×10^5) were treated for 8 h with 5 μM of SAHA or compound **2** in 10% FBS-supplemented McCoy's 5A medium and then collected and extracted with SDS buffer. Protein concentrations of the lysates were determined using a Bradford protein assay kit (Bio-Rad Laboratories); equivalent amounts of proteins from each lysate were resolved in 15% SDS–polyacrylamide gel and then transferred onto nitrocellulose membranes (Bio-Rad Laboratories). After blocking for 30 min with Tris-buffered saline (TBS) containing 3% skim milk, the transblotted membrane was incubated overnight at 4 °C with hyperacetylated histone H4 antibody (Upstate Biotechnology) (1:4000 dilution) in TBS containing 3% skim milk. After probing with the primary antibody, the membrane was washed twice with water, then incubated with goat anti-rabbit IgG-horseradish peroxidase conjugates (diluted 1:5000) for 2 h at room temperature, and further washed twice with water. The immunoblots were visualized by enhanced chemiluminescence.
18. NCH-51 and compound **2** (100 μM) were incubated at 37 °C in human plasma. The percentage of the parent compound remaining (%*R*) was determined by HPLC.

Available online at www.sciencedirect.com

ScienceDirect

Bioorganic & Medicinal Chemistry Letters

ELSEVIER

Bioorganic & Medicinal Chemistry Letters 17 (2007) 2055–2058

Novel mitochondria-localizing TEMPO derivative for measurement of cellular oxidative stress in mitochondria

Shizuka Ban, Hidehiko Nakagawa,* Takayoshi Suzuki and Naoki Miyata*

Graduate School of Pharmaceutical Sciences, Nagoya City University, 3-1 Tanabe-dori, Mizuho-ku, Nagoya, Aichi 467-8603, Japan

Received 20 November 2006; revised 30 December 2006; accepted 5 January 2007
Available online 17 January 2007

Abstract—Neurodegenerative disorders, such as Alzheimer's and Parkinson's diseases, and apoptosis, are thought to be associated with oxidative stress affecting mitochondria. In this study, we designed and synthesized a fluorescein-tagged TEMPO derivative, compound **1**, with triphenylphosphino moiety. Synthesized **1** localized in mitochondria and detected oxidative stress in an endotoxic model of a mouse macrophage-like cell line. Compound **1** is therefore a potentially useful probe for evaluating oxidative stress in mitochondria.

Oxygen taken into our bodies is used to produce energy, and about 1% of oxygen is transformed into reactive oxygen species (ROS). ROS are considered to play important roles; for instance, they serve as protective factors in inflammation, and they work as neuromodulators.[1] It is known that a variety of functions of cellular components, such as lipids, proteins, sugars, and DNA, suffer from oxidative stress when ROS are produced in excess.[2] Superoxide can be produced by electron transfer in mitochondria, and thus oxidative damage may accumulate more rapidly in mitochondria.[3] Oxidative stress affecting mitochondria is considered to be closely related to neurodegenerative disorders,[4] such as Alzheimer's[5] and Parkinson's diseases,[6] and apoptosis.[7]

However, there have been only a few attempts to measure the oxidative stress induced by ROS in specific cellular regions.[8] ROS can be measured indirectly by means of their reaction with stable radical compounds in the cell, through which radical probes are readily reduced to non-radical species.[9]

Among these radical species, 2,2,6,6-tetramethylpiperidin-1-oxyl (TEMPO) can be reduced to 2,2,6,6-tetramethylpiperidin-1-ol under physiological conditions, that is, TEMPO converts to the non-radical form by reduction.[10] When ROS are upregulated and cells are in a relatively oxidative environment, cellular reduction will be downregulated. Electron spin resonance (ESR) measurement is a useful approach to detect radical species in biological systems. Using TEMPOL (4-hydroxyl-2,2,6,6-tetramethylpiperidin-1-oxyl), a useful TEMPO derivative, oxidative stress can be measured by ESR spectrometry. TEMPOL is easily introduced into cells, but, due to its amphiphilic nature, can easily exit cells as well.[11] TEMPO derivatives, which localize to a particular cellular region, would be useful for measuring regional oxidative stress, such as stress at mitochondria. A TEMPO derivative localizing to mitochondria would be advantageous.

For this purpose, the TEMPO derivative requires a radical moiety for ESR detection, a fluorescent group for identifying its cellular distribution, and a functional group for localizing to a particular region. We have already developed such probes localizing to the cell membrane and succeeded in evaluating oxidative stress at the cell membrane.[12]

In this study, we designed a TEMPO derivative (Fig. 1), that has a cationic triphenylphosphonium moiety for localization to the mitochondria,[13] nitroxyl radical moiety for measuring ESR, and fluorescein moiety for confirming distribution in cells. Compound **1** was synthesized as shown in Scheme 1, and we demonstrated that this radical probe was able to detect oxidative stress in mitochondria in an endotoxic model of a mouse macrophage-like cell line.

Keywords: Fluorescein; Redox; Electron spin resonance; Reactive oxygen species; Superoxide; Inflammation.
* Corresponding authors. Tel./fax: +81 52 836 3407; e-mail addresses: deco@phar.nagoya-cu.ac.jp; miyata-n@phar.nagoya-cu.ac.jp

0960-894X/$ - see front matter © 2007 Elsevier Ltd. All rights reserved.
doi:10.1016/j.bmcl.2007.01.011

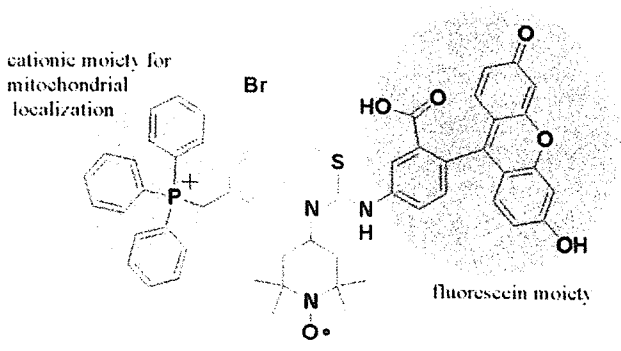

1

Figure 1. Structure of a TEMPO derivative (1) designed to localize to mitochondria.

Mouse RAW264.7 cells were cultured in DMEM culture medium containing penicillin and streptomycin, supplemented with fetal bovine serum. For the experiments, the cells were plated onto 10-cm culture dishes at 1.5×10^7 cells/dish with 15 mL of DMEM culture medium. The cells were incubated at 37 °C in a humidified 5% (v/v) CO_2 incubator for 2 days. Then, the culture medium was replaced with 5 mL of serum-free DMEM, and the cells were treated with LPS (*Escherichia coli*, 0.5 μg/mL) and IFN-γ (human recombinant, 150 U/mL). The treated cells were subsequently cultured for 5 h, scraped into 2 mL of Dulbecco's PBS (D-PBS), and washed with D-PBS. Then the cells were treated with 50 μM of **1** for 15 min under dark conditions, followed by washing 3 times with D-PBS. The cell suspension (1 mL) was used for the ESR experiments. There was no significant difference in cell number between non-treated- and LPS/IFN-γ-treated cell suspension (supporting information).

Each suspension of the treated cells was placed in a flat quartz cuvette. ESR measurements were started 10 min after treatment with **1**. The ESR signal was recorded at 5-min intervals. The signal intensity of TEMPO derivative (I) was calculated from the second integral of the center peak of the signal trace and expressed as a ratio (I/I_0) by comparing it to the intensity of the standard Mn^{2+} signal (I_0). The signal decay rate ($-k$) was calculated as the pseudo first order rate of the decrease in the ratio (I/I_0). For confocal microscopy, the cells were plated on a 3-cm glass-bottomed culture dish at 1.5×10^5 cells/dish with 1.5 mL of DMEM culture medium and incubated at 37 °C in a humidified 5% (v/v) CO_2 incubator for 2 days. The cells were treated with **1** in the same manner as in the ESR experiments without detachment. The cells were subsequently stained with MitoRed, which is known as a rhodamine-based well-established mitochondria dye, for 10 min and subjected to confocal fluorescence microscopy. The confocal microscopic study of the RAW264.7 cells treated with compound **1** indicated that **1** was localized to mitochondria as expected (Fig. 2). Its membrane-permeable cationic moiety probably contributed to the localization to mitochondria because mitochondria are negatively charged compared with cytosol. The ESR signal of **1** was measured in RAW264.7 cells to evaluate oxidative stress in mitochondria (Figs. 3 and 4). In the control cells, the signal intensity of **1** was gradually decreased at $0.0080 \pm 0.0004\ min^{-1}$ under our conditions. The upregulation of oxidative stress was evaluated after endotoxic stimulation (Fig. 4a). ESR spectra of **1** were measured in RAW264.7 cells, which had been treated with 500 ng/mL LPS and 150 U/mL IFN-γ for 5 h. The rate of signal decay observed in cells treated with LPS/IFN-γ was decreased to $0.0063 \pm 0.0009\ min^{-1}$. The decreased rate as a result of the LPS/IFN-γ treatment was restored to $0.0077 \pm 0.0007\ min^{-1}$ in the presence of 100 U/mL SOD and 10 U/mL catalase during measurement (Fig. 4b).

In the absence of the RAW264.7 cells, the signal failed to decay (data not shown). Since cells generally exist in a reductive environment, compound **1** was found to be gradually reduced to the non-radical species in the presence of the control cells.

Treatment with LPS/IFN-γ is known to activate the cells and to increase the production of reactive oxygen and nitrogen species (ROS/RNS). In this study, LPS/IFN-γ treatment decreased the decay rate of nitroxyl radical. The decrease in the rate was recovered in the presence of 100 U/mL SOD and 10 U/mL catalase. Although ROS were still upregulated by LPS/IFN-γ treatment, they were considered to be at least partially scavenged by SOD and catalase. These two enzymes seem to contribute to reduce ROS around the mitochondria by scavenging around cells, although these enzymes may be incapable of approach to mitochondria. LPS/IFN-γ treatment is known to increase ROS production by activating NADPH oxidase on endosomes. One possibility is that SOD and catalase may scavenge ROS around the cell membrane and reduce total ROS, so that the population of ROS diffusing to mitochondria may be

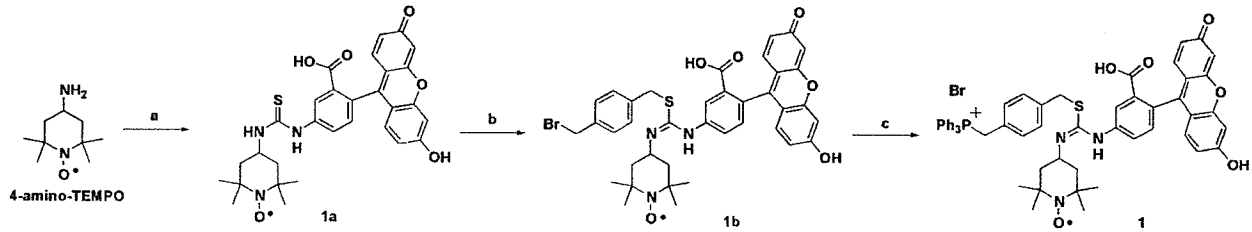

Scheme 1. Synthesis of compound **1**. Reagents and conditions: (a) fluorescein-5-isothiocyanate, THF, 87%; (b) α,α′-dibromo-*p*-xylene, $NaHCO_3$, DMF, 44%; (c) PPh_3, AcOEt, 94%.

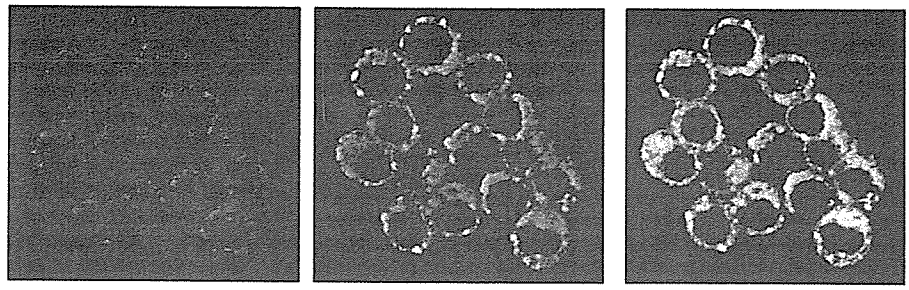

Figure 2. RAW264.7 cells were stained simultaneously with MitoRed and compound **1**, and observed by confocal fluorescence microscopy. Distribution of MitoRed (left, red), distribution of compound **1** (center, green), and merged image (right) at same field are shown.

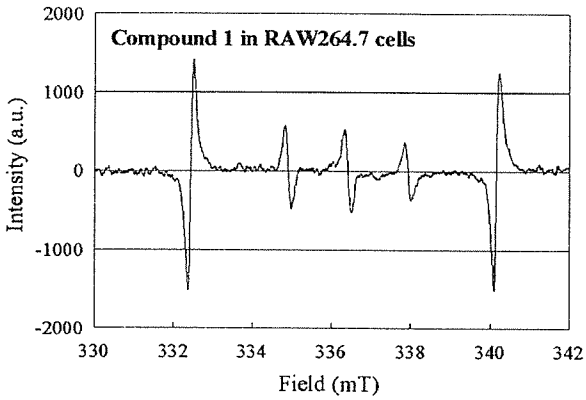

Figure 3. ESR spectra were recorded with a JES-RE 2X spectrometer (JEOL Co. Ltd., Tokyo, Japan). The settings used were as follows: microwave power, 10 mW; frequency, 9.42 GHz; field, 336.5 mT; sweep width, 7.5 mT; sweep time, 1 min; modulation width, 0.063 mT; gain, 2500; and time constant, 0.03. The signal intensity of TEMPO derivative (I) was calculated from the second integral of the signal trace and expressed as a ratio (I/I_0) by comparing it to the intensity of the standard Mn^{2+} signal (I_0).

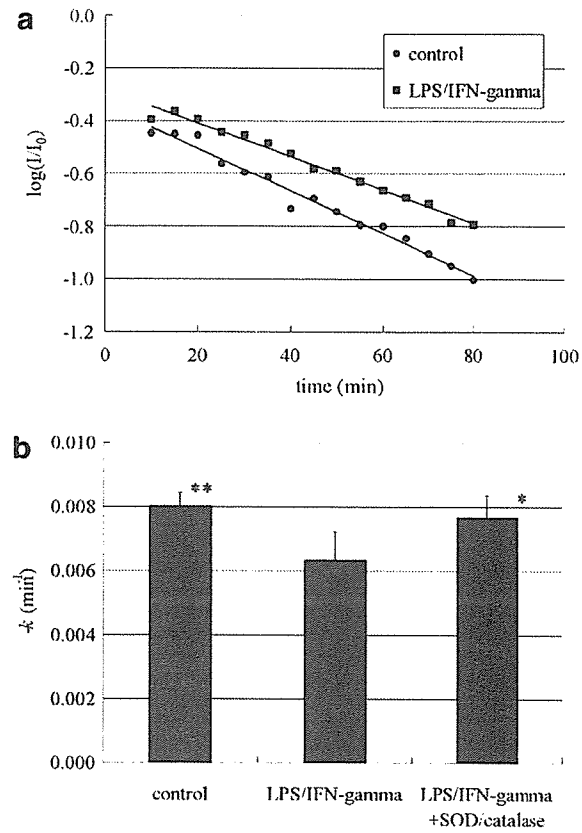

Figure 4. Signal decay rate of compound **1** in RAW264.7 cells. (a) The time course of the relative signal intensity measured at 5-min intervals, control cells (•), LPS/IFN-γ-treated cells (■). I, compound **1** peak area; I_0, Mn^{2+} external standard peak area. (b) Signal decay rate of **1** in RAW264.7 cells. The signal decay rates of **1** with RAW264.7 cells were calculated from ESR signal intensities of **1** in RAW264.7 cells treated with vehicle, or with LPS/IFN-γ, in the presence or absence of SOD/catalase. Values are presented as means ± SD of 4–7 experiments. ANOVA and Bonferroni-type multiple t test indicated significant differences between LPS/IFN-γ and the control ($^{**}P < 0.01$), and LPS/IFN-γ + SOD/catalase ($^{*}P < 0.05$).

also decreased. The change in this rate after LPS/IFN-γ-treatment was assumed to be due to either a decrease in the cellular reductants by ROS upregulation or an increase in the oxidation of hydroxylamine, a reduced form of **1**.[14] The TEMPO moiety can be oxidized to the ESR-silent oxonium cation formed by superoxide.[15] However, this cation was known to be rapidly reduced back to TEMPO by superoxide itself.[15] Compound **1** might be considered to be repeatedly oxidized and reduced in mitochondria. The direct oxidation of TEMPO itself by superoxide probably does not affect the signal decay rate under the conditions used for these measurements.

Cells generally exist in a reductive environment, and radical compounds are reduced to non-radical species by intracellular reductants such as glutathione. Reductant concentration is considered to be kept at a constant value ($[Red]_{const}$) in a living cell (Eq. 1) by homeostasis.

When treated with LPS/IFN-γ, ROS/RNS are upregulated, and reductants are consumed to reduce ROS/RNS in a cell, so that the intracellular reductant concentration is considered to be shifted to a smaller constant value ($[Red]'_{const}$), at which reductant consumption and regeneration are balanced. Therefore, the reducing rate of a TEMPO derivative would be decreased as shown in Eqs. 2 and 3. Here, [T·] is for TEMPO radical concentration, [Red] is for reductant concentration, k and k_{obs} are for rate constant and observed pseudo first order rate constant, respectively.

In untreated cells

$$-d[T\cdot]/dt = k[Red]_{const}[T\cdot] = k_{obs}[T\cdot]. \quad (1)$$

In treated cells

$$-d[T\cdot]/dt = k[Red]'_{const}[T\cdot] = k'_{obs}[T\cdot] \quad (2)$$

$$k_{obs} > k'_{obs} (\text{when } [Red]_{const} > [Red]'_{const}). \quad (3)$$

The difference in reducing rate of [T·] reflects the difference between k_{obs} and k'_{obs}. The difference between k_{obs} and k'_{obs} comes from the difference between $[Red]_{const}$ and $[Red]'_{const}$. Since the change of $[Red]_{const}$ (to $[Red]'_{const}$) is dependent on the generation of ROS/RNS, it is assumed to reflect the concentration of ROS/RNS. Both k_{obs} and k'_{obs} do not include the term [T·], so that the rates are able to be compared to each other without consideration of the difference in initial concentration of the radicals. Direct oxidation of the hydroxylamine, the reduced form of **1**, by ROS may also contribute to the decrease of the decay rate of **1** in LPS/IFN-γ-treated cells.[16] This reaction is also slowed by the reduction of ROS/RNS in the presence of SOD and catalase, indicating a recovery of the decay rate.

In comparison with the decay rate measured at cell membrane using a membrane-localizing probe reported previously,[12] the change of the decay rate of the probe in mitochondria is smaller than that in the cell membrane by LPS/IFN-γ treatment. It is assumed that mitochondria have intense reducing ability or produced lesser amounts of ROS/RNS than cell membranes with LPS/IFN-γ treatment. These results suggest that oxidative damage in mitochondria is smaller than in the cell membrane in this endotoxic model. Since NADPH oxidase is upregulated near the cell membrane in this model, it is consistent that the decay rate in cell membrane is significantly larger than in mitochondria.

In conclusion, compound **1** was found to be a useful probe for evaluating oxidative stress in mitochondria.

Supplementary data

Supplementary data associated with this article can be found, in the online version, at doi:10.1016/j.bmcl.2007.01.011.

References and notes

1. (a) Irani, K.; Goldschmidt-Clermont, P. J. *Biochem. Pharmacol.* **1998**, *55*, 1339; (b) Irani, K.; Xia, Y.; Zweier, J. L.; Sollott, S. J.; Der, C. J.; Fearon, E. R.; Sundaresan, M.; Finkel, T.; Goldschmidt-Clermont, P. J. *Science* **1997**, *275*, 1649.
2. Darley-Usmar, V.; Halliwell, B. *Pharm. Res.* **1996**, *13*, 649.
3. (a) Liu, Y.; Fiskum, G.; Schubert, D. *J. Neurochem.* **2002**, *80*, 780; (b) Lenaz, G. *Biochem. Biophys. Acta* **1998**, *1366*, 53.
4. (a) Halliwell, B. *J. Neurochem.* **2006**, *96*, 1634; (b) Beal, M. F. *Ann. Neurol.* **2005**, *58*, 495; (c) Emerit, J.; Edeas, M.; Bricaire, F. *Biomed. Pharmacother.* **2004**, *58*, 39.
5. (a) Nunomura, A.; Castellani, R. J.; Zhu, X.; Moreira, P. I.; Perry, G.; Smith, M. A. *J. Neuropathol. Exp. Neurol.* **2006**, *65*, 631; (b) Eckert, A.; Keil, U.; Marques, C. A.; Bonert, A.; Frey, C.; Schussel, K.; Muller, W. E. *Biochem. Pharmacol.* **2003**, *66*, 1627.
6. (a) Jenner, P. *Ann. Neurol.* **2003**, *53*, 26; (b) Fiskum, G.; Starkov, A.; Polster, B. M.; Chinopoulos, C. *Ann. N.Y. Acad. Sci.* **2003**, *991*, 111.
7. Zhao, K.; Luo, G.; Giannelli, S.; Szeto, H. H. *Biochem. Pharmacol.* **2005**, *70*, 1796.
8. (a) Wipf, P.; Xiao, J.; Jiang, J.; Belikova, N. A.; Tyurin, V. A.; Fink, M. P.; Kagan, V. E. *J. Am. Chem. Soc.* **2005**, *127*, 12460; (b) Okamoto, A.; Inasaki, T.; Saito, I. *Bioorg. Med. Chem. Lett.* **2004**, *14*, 3415; (c) Freedman, J. E.; Keaney, JF., Jr. *Methods Enzymol.* **1999**, *301*, 61.
9. Nakagawa, H.; Moritake, T.; Tsuboi, K.; Ikota, N.; Ozawa, T. *FEBS Lett.* **2000**, *471*, 187.
10. (a) May, J. M.; Qu, Z. C.; Juliao, S.; Cobb, C. E. *Free Radical Res.* **2005**, *39*, 195; (b) Iannone, A.; Bini, A.; Swartz, H. M.; Tomasi, A.; Vannini, V. *Biochem. Pharmacol.* **1989**, *38*, 2581.
11. Cuzzocrea, S.; McDonald, M. C.; Mazzon, E.; Dugo, L.; Lepore, V.; Fonti, M. T.; Ciccolo, A.; Terranova, M. L.; Caputi, A. P.; Thiemerann, C. *Eur. J. Pharmacol.* **2000**, *406*, 127.
12. Ban S.; Nakagawa H.; Suzuki T., Miyata N. *Bioorg. Med. Chem. Lett.* **2007**, doi: 10.1016/j.bmcl.2006.11.040.
13. Coulter, C. V.; Kelso, G. F.; Lin, T. K.; Smith, R. A.; Murphy, M. P. *Free Radical Biol. Med.* **2000**, *28*, 1547.
14. Zigler, J. S., Jr.; Qin, C.; Kamiya, T.; Krishna, M. C.; Cheng, Q.; Tumminia, S.; Russell, P. *Free Radical Biol. Med.* **2003**, *35*, 1194.
15. Krishna, M. C.; Russo, A.; Mitchell, J. B.; Goldstein, S.; Dafni, H.; Samuni, A. *J. Biol. Chem.* **1996**, *271*, 26026.
16. Samuni, A.; Goldstein, S.; Russo, A.; Mitchell, J. B.; Krishna, M. C.; Neta, P. *J. Am. Chem. Soc.* **2002**, *124*, 8719.

Journal of Cellular Physiology

Granulocyte Colony-Stimulating Factor Promotes the Translocation of Protein Kinase Cι in Neutrophilic Differentiation Cells

TOSHIE KANAYASU-TOYODA,[1] TAKAYOSHI SUZUKI,[1] TADASHI OSHIZAWA,[1] ERIKO UCHIDA,[2] TAKAO HAYAKAWA,[2] AND TERUHIDE YAMAGUCHI[1]*

[1]*Division of Cellular and Gene Therapy Products, National Institute of Health Sciences, Tokyo, Japan*

[2]*National Institute of Health Sciences, Tokyo, Japan*

Previously, we suggested that the phosphatidylinositol 3-kinase (PI3K)-p70 S6 kinase (p70 S6K) pathway plays an important role in granulocyte colony-stimulating factor (G-CSF)-dependent enhancement of the neutrophilic differentiation and proliferation of HL-60 cells. While atypical protein kinase C (PKC) has been reported to be a regulator of p70 S6K, abundant expression of PKCι was observed in myeloid and lymphoid cells. Therefore, we analyzed the participation of PKCι in G-CSF-dependent proliferation. The maximum stimulation of PKCι was observed from 15 to 30 min after the addition of G-CSF. From 5 to 15 min into this lag time, PKCι was found to translocate from the nucleus to the membrane. At 30 min it re-translocated to the cytosol. This dynamic translocation of PKCι was also observed in G-CSF-stimulated myeloperoxidase-positive cells differentiated from cord blood cells. Small interfering RNA for PKCι inhibited G-CSF-induced proliferation and the promotion of neutrophilic differentiation of HL-60 cells. These data indicate that the G-CSF-induced dynamic translocation and activation processes of PKCι are important to neutrophilic proliferation.

J. Cell. Physiol. 211: 189–196, 2007. © 2006 Wiley-Liss, Inc.

Hematopoietic cell differentiation is regulated by a complex network of growth and differentiation factors (Tenen et al., 1997; Ward et al., 2000). Granulocyte colony-stimulating factor (G-CSF) and its receptors are pivotal to the differentiation of myeloid precursors into mature granulocytes. In previous studies (Kanayasu-Toyoda et al., 2002) on the neutrophilic differentiation of HL-60 cells treated with either dimethyl sulfoxide (DMSO) or retinoic acid (RA), heterogeneous transferrin receptor (Trf-R) populations—transferrin receptor-positive (Trf-R$^+$) cells and transferrin receptor-negative (Trf-R$^-$) cells—appeared 2 days after the addition of DMSO or RA. The Trf-R$^+$ cells were proliferative-type cells that had higher enzyme activity of phosphatidylinositol 3-kinase (PI3K) and protein 70 S6 kinase (p70 S6K), whereas the Trf-R$^-$ cells were differentiation-type cells of which Tyr705 in STAT3 was much more phosphorylated by G-CSF. Inhibition of either PI3K by wortmannin or p70 S6K by rapamycin was found to eliminate the difference in differentiation and proliferation abilities between Trf-R$^+$ and Trf-R$^-$ cells in the presence of G-CSF (Kanayasu-Toyoda et al., 2002). From these results, we concluded that proteins PI3K and p70 S6K play important roles in the growth of HL-60 cells and negatively regulate neutrophilic differentiation. On the other hand, the maximum kinase activity of PI3K was observed at 5 min after the addition of G-CSF (Kanayasu-Toyoda et al., 2002) and that of p70 S6K was observed between 30 and 60 min after, indicating a lag time between PI3K and p70 S6K activation. It is conceivable that any signal molecule(s) must transduce the G-CSF signal during the time lag between PI3K and p70 S6K. Chung et al. (1994) also showed a lag time between PI3K and p70 S6K activation on HepG2 cells stimulated by platelet-derived growth factor (PDGF), suggesting that some signaling molecules also may transduce between PI3K and p70S6K.

Protein kinase C (PKC) is a family of Ser/Thr kinases involved in the signal transduction pathways that are triggered by numerous extracellular and intracellular stimuli. The PKC family has been shown to play an essential role in cellular functions, including mitogenic signaling, cytoskeleton rearrangement, glucose metabolism, differentiation, and the regulation of cell survival and apoptosis. Eleven different members of the PKC family have been identified so far. Based on their structural similarities and cofactor requirements, they have been grouped into three subfamilies: (1) the classical or conventional PKCs (cPKCα, β_1, β_2, and γ), activated by Ca^{2+}, diacylglycerol, and phosphatidyl-serine; (2) the novel PKCs (nPKCδ, ε, η, and θ), which are independent of Ca^{2+} but still responsive to diacylglycerol; and (3) the atypical PKCs (aPKCζ and ι/λ), where PKCλ is the homologue of human PKCι. Atypical PKCs differ significantly from all other PKC family

Abbreviations: DMSO, dimethyl sulfoxide; fMLP-R, formyl-Met-Leu-Phe receptor; RA, retinoic acid; G-CSF, granulocyte colony-stimulating factor; Trf-R, transferrin receptor; BSA, bovine serum albumin; FITC, fluorescein isothiocyanate; PBS, phosphate-buffered saline; PKC, protein kinase C; PI3K, phosphatidylinositol 3-kinase; p70 S6K, protein 70 S6 kinase; SDS–PAGE, sodium dodecyl sulfate-polyacrylamide gel electrophoresis; siRNA, small interfering RNA; PMN, polymorphonuclear leukocyte.

Contract grant sponsor: Ministry of Health, Labor, and Welfare of Japan.
Contract grant sponsor: Ministry of Education, Culture, Sports, Science, and Technology of Japan.

*Correspondence to: Teruhide Yamaguchi, Division of Cellular and Gene Therapy Products, National Institute of Health Sciences, 1-18-1, Kamiyoga, Setagaya-ku, Tokyo 158-8501, Japan.
E-mail: yamaguch@nihs.go.jp

Received 31 May 2006; Accepted 22 September 2006

Published online in Wiley InterScience (www.interscience.wiley.com.), 28 November 2006.
DOI: 10.1002/jcp.20930

members in their regulatory domains, in that they lack both the calcium-binding domain and one of the two zinc finger motifs required for diacylglycerol binding (Liu and Heckman, 1998). Romanelli et al. (1999) reported that p70 S6K is regulated by PKCζ and participates in a PI3K-regulated signaling complex. On the other hand, Selbie et al. (1993) reported that the tissue distribution of PKCζ is different from that of PKCι/λ, and that PKCι/λ appears to be widely expressed. If the p70 S6K could be activated by aPKC, the regulation of p70 S6K activation would seem to depend on the tissue-specific expression of PKCι and/or PKCζ. In neutrophilic lineage cells, the question is which aPKC participates in the regulation of p70 S6K on G-CSF signaling.

In this study, we show that G-CSF activated PKCι, promoting its translocation from the nucleus to the cell surface membrane and subsequently to the cytosol in DMSO-treated HL-60 cells. We also show the translocation of PKCι using myeloperoxidase-positive neutrophilic lineage differentiated from cord blood, which is a rich source of immature myeloid cells (Fritsch et al., 1993; Rappold et al., 1997; Huang et al., 1999; Debili et al., 2001; Hao et al., 2001). We concluded that PKCι translocation and activation by G-CSF are needed for neutrophilic proliferation.

Materials and Methods

Reagents

Anti-p70 S6K polyclonal antibody was obtained from Santa Cruz Biotechnology (Santa Cruz, CA). Anti-PKCι polyclonal antibody and monoclonal antibody were purchased from Santa Cruz Biotechnology and from Transduction Laboratories (Lexington, KY), respectively. Anti-PKCζ polyclonal antibody was purchased from Cell Signaling Technology (Beverly, MA). Anti-myeloperoxidase antibody was purchased from Serotec Ltd. (Oxford, UK). GF 109203X, and Gö 6983 were obtained from Calbiochem-Novabiochem (San Diego, CA). Wortmannin was obtained from Sigma Chemical (St. Louis, MO). Anti-Histon-H1 antibody, anti-Fcγ receptor IIa (CD32) antibody, and anti-lactate dehydrogenase antibody were from Upstate Cell Signaling Solutions (Lake Placid, NY), Lab Vision Corp. (Fremont, CA), and Chemicon International, Inc. (Temecula, CA), respectively.

Cell culture

HL-60, Jurkut, K562, U937, and THP-1 cells were kindly supplied by the Japanese Collection of Research Bioresources Cell Bank (Osaka, Japan). Cells were maintained in RPMI 1640 medium containing 10% heat-inactivated FBS and 30 mg/L kanamycin sulfate at 37°C in moisturized air containing 5% CO_2. The HL-60 cells, which were at a density of 2.5×10^5 cells/ml, were differentiated by 1.25% DMSO. Two days after the addition of DMSO, the G-CSF-induced signal transduction was analyzed using either magnetically sorted cells or non-sorted cells.

Magnetic cell sorting

To prepare Trf-R$^-$ and Trf-R$^+$ cells, magnetic cell sorting was performed as previously reported (Kanayasu-Toyoda et al., 2002), using an automatic cell sorter (AUTO MACS; Miltenyi Biotec, Bergisch Gladbach, Germany). After cell sorting, both cell types were used for Western blotting and PKCι enzyme activity analyses.

Preparation of cell lysates and immunoblotting

For analysis of PKCι and PKCζ expression, a PVDF membrane blotted with 50 μg of various tissues per lane was purchased from BioChain Institute (Hayward, CA). Both a polymorphonuclear leukocytes (PMNs) fraction and a fraction containing lymphocytes and monocytes were isolated by centrifugation (400g, 25 min) using a Mono-poly resolving medium (Dai-Nippon Pharmaceutical, Osaka, Japan) from human whole blood, which was obtained from a healthy volunteer with informed consent. T-lymphocytes were further isolated from the mixture fraction using the Pan T Cell Isolation Kit (Miltenyi Biotec) according to the manufacturer's protocol. T-lymphocytes, PMNs, HL-60 cells, Jurkut cells, K562 cells, and U937 cells (1×10^7) were collected and lysed in lysis buffer containing 1% Triton X-100, 10 mM K_2HPO_4/KH_2PO_4 (pH 7.5), 1 mM EDTA, 5 mM EGTA, 10 mM $MgCl_2$, and 50 mM β-glycerophosphate, along with 1/100 (v/v) protease inhibitor cocktail (Sigma Chemical) and 1/100 (v/v) phosphatase inhibitor cocktail (Sigma Chemical). The cellular lysate of 10^6 cells per lane was subjected to Western blotting analysis. Human cord blood was kindly supplied from the Metro Tokyo Red Cross Cord Blood Bank (Tokyo, Japan) with informed consent. Mononuclear cells, isolated with the Lymphoprep™ Tube (Axis-Shield PoC AS, Oslo, Norway), were cultured in RPMI 1640 medium containing 10% FBS in the presence of G-CSF for 3 days. Cultured cells were collected, and the cell lysate was subjected to Western blotting analysis.

A fraction of the plasma membrane, cytosol, and nucleus of the DMSO-treated HL-60 cells was prepared by differential centrifugation after the addition of G-CSF, as described previously (Yamaguchi et al., 1999). After the cells that had been suspended in 250 mM sucrose/10 mM Tris-HCl (pH 7.4) containing 1/100 (v/v) protease inhibitor cocktail (Sigma Chemical) were gently disrupted by freezing and thawing, they were centrifuged at 800g, 4°C for 10 min. The precipitation was suspended in 10 mM Tris-HCl (pH 6.7) supplemented with 1% SDS. It was then digested by benzon nuclease at 4°C for 1 h and used as a sample of the nuclear fraction. After the post-nucleus supernatant was re-centrifuged at 100,000 rpm (452,000g) at a temperature of 4°C for 40 min, the precipitate was used as a crude membrane fraction and the supernatant as a cytosol fraction. Western blotting analysis was then performed as described previously (Kanayasu-Toyoda et al., 2002). The bands that appeared on x-ray films were scanned, and the density of each band was quantitated by Scion Image (Scion, Frederick, MD) using the data from three separate experiments.

Kinase assay

The activity of PKCι was determined by phosphorous incorporation into the fluorescence-labeled pseudosubstrate (Pierce Biotechnology, Rockford, IL). The cell lysates were prepared as described above and immunoprecipitated with the anti-PKCι antibody. Kinase activity was measured according to the manufacturer's protocol. In the analysis of inhibitors effects, cells were pretreated with a PI3K inhibitor, wortmannin (100 nM), or PKC inhibitors, GF109207X (10 μM) and Gö6983 (10 μM) for 30 min, and then stimulated by G-CSF for 15 min.

Observation of confocal laser-scanning microscopy

Upon the addition of G-CSF, PKCι localization in the DMSO-treated HL-60 cells for 2 days was examined by confocal laser-activated microscopy (LSM 510, Carl Zeiss, Oberkochen, Germany). The cells were treated with 50 ng/ml G-CSF for the indicated periods and then fixed with an equal volume of 4.0% paraformaldehyde in PBS(−). After treatment with ethanol, the fixed cells were labeled with anti-PKCι antibody and with secondary antibody conjugated with horseradish peroxidase. They were then visualized with TSA™ Fluorescence Systems (PerkinElmer, Boston, MA).

Mononuclear cells prepared from cord blood cells were cultured in RPMI 1640 medium containing 10% FBS in the presence of G-CSF for 7 days. Then, for serum and G-CSF starvation, cells were cultured in RPMI 1640 medium containing 1% BSA for 11 h. After stimulation by 50 ng/ml G-CSF, the cells were fixed, stained with both anti-PKCι polyclonal antibody and anti-myeloperoxidase monoclonal antibody, and finally visualized with rhodamine-conjugated anti-rabbit IgG and FITC-conjugated anti-mouse IgG, respectively.

RNA interference

Two pairs of siRNAs were chemically synthesized: annealed (Dharmacon RNA Technologies, Lafayette, CO) and transfected into HL-60 cells using Nucleofector™ (Amaxa, Cologne, Germany). The sequences of sense siRNAs were as follows: PKCι, GAAGAAGCCUUUAGACUUUTA; p70 S6K, GCAAGGAGUCUAUCCAUGAUU. As a control, the sequence ACUCUAUCGCCAGCGUGACUU was used. Forty-eight hours after treatment with siRNA, the cells were lysed for Western blot analysis. For proliferation and differentiation assay, cells were transfected with siRNA on the first day, treated with DMSO on the second day, and supplemented with G-CSF on the third day. After cells were subsequently cultured for 5 days, cell numbers and formyl-Met-Leu-Phe receptor (fMLP-R) expression were determined.

fMLP-R expression

The differentiated cells were collected and incubated with FITC-conjugated fMLP; then, labeled cells were subjected to flow cytometric analysis (FACSCalibur, Becton Dickinson, Franklin Lakes, NJ).

Statistical analysis

Statistical analysis was performed using unpaired Student's *t*-test. Values of $P < 0.05$ were considered to indicate statistical significance. Each experiment was repeated at least three times and representative data were indicated.

Results

The distribution of atypical PKC in various tissues and cells

Previously, we reported that the PI3K-p70 S6K-cMyc pathway plays an important role in the G-CSF-induced proliferation of DMSO-treated HL-60 cells, not only by enhancing the activity of both PI3K and p70 S6K but also by inducing the c-Myc protein (Kanayasu-Toyoda et al., 2002, 2003). We also reported that G-CSF did not stimulate Erk1, Erk2, or 4E-binding protein 1. The maximum kinase activity of PI3K was observed 5 min after the addition of G-CSF, and that of p70 S6K was observed between 30 and 60 min after. It is conceivable that any signal molecule(s) must transduce the G-CSF signal during the time lag between PI3K and p70 S6K. Romanelli et al. (1999) suggested that the activation of p70 S6K is regulated by PKCξ and participates in the PI3K-regulated signaling complex. To examine the role of atypical PKC in the G-CSF-dependent activation and the relationship between atypical PKC and p70 S6K, the protein expression of PKCζ and PKCι in various human tissues and cells was analyzed by Western blotting. As shown in Figure 1A, both of the atypical PKCs were markedly expressed in lung and kidney but were weakly expressed in spleen, stomach, and placenta. In brain, cervix, and uterus, the expression of only PKCι was observed. Selbie et al. (1993) have reported observing the expression of PKCζ not in protein levels but in RNA levels, in the kidney, brain, lung, and testis, and that of PKCι in the kidney, brain, and lung. In this study, the protein expression of PKCι in the kidney, brain, and lung was consistent with the RNA expression of PKCι. Despite the strong expression of PKCζ RNA in brain (Selbie et al., 1993), PKCζ protein was scarcely observed. Although PKCι proteins were scarcely expressed in neutrophils and T-lymphocytes in peripheral blood, they were abundantly expressed in immature blood cell lines, that is, Jurkut, K562, U937, and HL-60 cells (Fig. 1B), in contrast with the very low expression of PKCζ proteins. In mononuclear cells isolated from umbilical cord blood, which contains large numbers of immature myeloid cells and has a high proliferation ability, the expression of PKCι proteins was also observed. Since Nguyen and Dessauer (2005) have reported observing abundant PKCζ proteins in THP-1 cells, as a positive control for PKCζ, we also performed a Western blot of THP-1 cells (Fig. 1B, right part). While PKCι was markedly expressed in both THP-1 and HL-60 cells, PKCζ was observed only in THP-1 cells.

These data suggested that PKCζ and PKCι were distributed differently in various tissues and cells, and that mainly PKCι proteins were expressed in proliferating blood cells.

Stimulation of PKCι activity by G-CSF

Among the 11 different members of the PKC family, the aPKCs (ζ and ι/λ) have been reported to activate p70 S6K activity and to be regulated by PI3K (Akimoto et al., 1998; Romanelli et al., 1999). As shown in Figure 1, although the PKCζ proteins were not detected by Western blotting in HL-60 cells or mononuclear cells isolated from cord blood cells, it is possible that PKCι could functionally regulate p70 S6K as an upstream

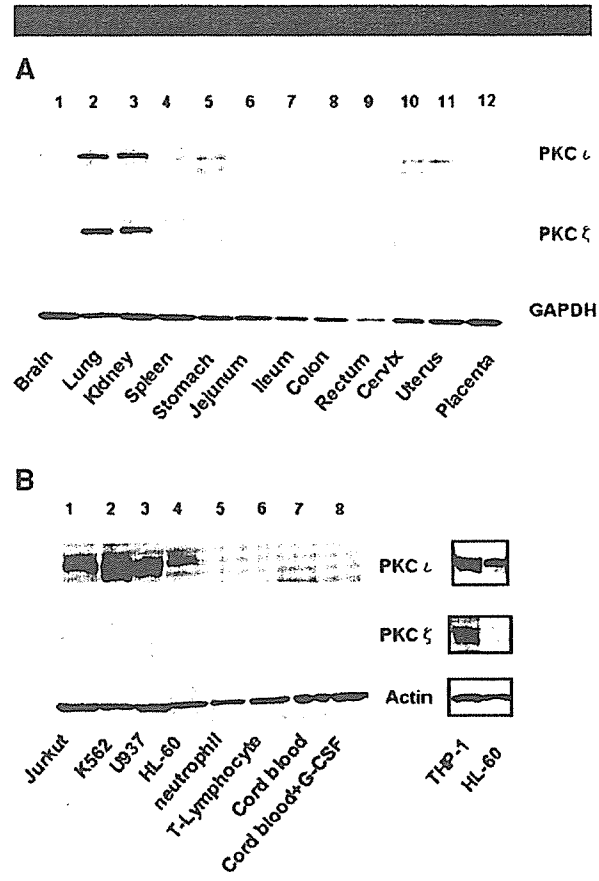

Fig. 1. Different distributions of PKCζ and PKCι. The protein expression of PKCι appears in the upper part and that of PKCζ in the middle part in various tissues and cells. A: 1, brain; 2, lung; 3, kidney, 4, spleen; 5, stomach; 6, jejunum; 7, ileum; 8, colon; 9, rectum; 10, cervix; 11, uterus; 12, placenta. Anti-GAPDH blot is a control for various tissues. B: 1, Jurkut cells; 2, K562 cells; 3, U937 cells; 4, HL-60 cells; 5, neutrophils; 6, T-lymphocytes; 7, mononuclear cells from cord blood in the absence of G-CSF; 8, mononuclear cells from cord blood in the presence of G-CSF. Anti-actin blot is a control. The right part shows immunoblots of PKCι, PKCζ, and actin of THP-1 cells as a positive control for PKCζ. The cell numbers of THP-1 and HL-60 cells were adjusted in relation to other cells on the left parts.

regulator in these cells. Therefore, we focused on the role of PKCι as the possible upstream regulator of p70 S6K in neutrophil lineage cells. First, we compared the expression of PKCι in both Trf-R$^-$ and Trf-R$^+$ cells. PKCι proteins were expressed more abundantly in Trf-R$^+$ cells than in Trf-R$^-$ cells (Fig. 2A, middle part), as with the p70 S6K proteins. A time course study of PKCι activity upon the addition of G-CSF revealed the maximum stimulation at 15 min, lasting until 30 min. The G-CSF-dependent activation of PKCι was inhibited by the PKC inhibitors wortmannin, GF 109203X, and Gö 6983. Considering the marked inhibitory effect of wortmannin on PKCι and evidence that the maximum stimulation of PI3K was observed at 5 min after the addition of G-CSF, PI3K was determined to be the upstream regulator of PKCι in the G-CSF signal transduction of HL-60 cells. The basal activity of PKCι in Trf-R$^+$ cells was higher than that in Trf-R$^-$ cells, and G-CSF was more augmented. In Trf-R$^-$ cells, PKCι activity was scarcely stimulated by G-CSF. This tendency of PKCι to be activated by G-CSF was similar to that of PI3K (Kanayasu-Toyoda et al., 2002).

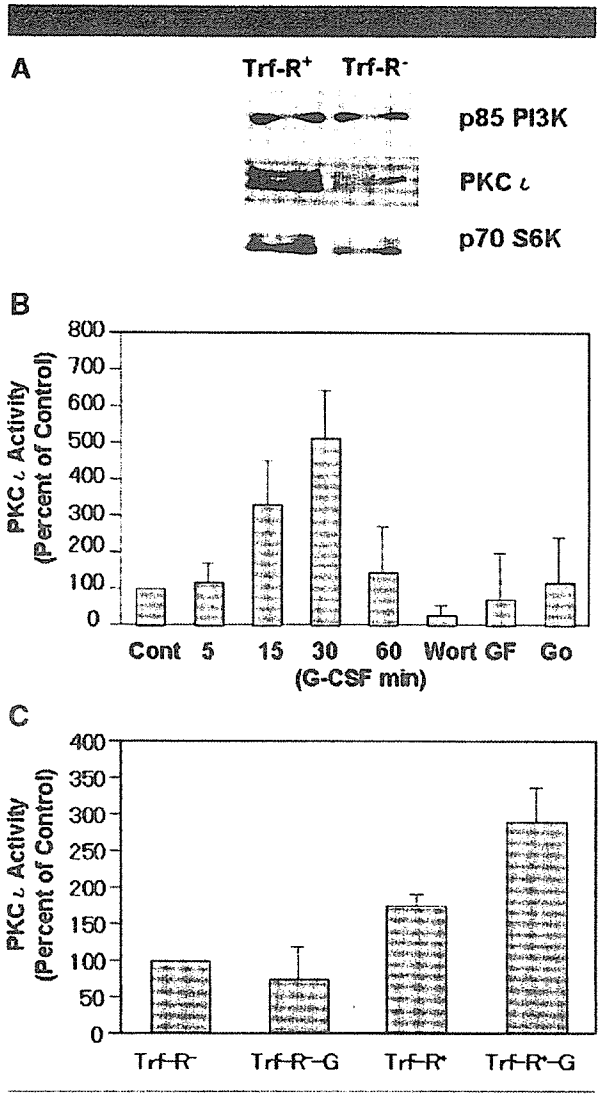

Fig. 2. Expression of PKCι in Trf-R$^+$ and Trf-R$^-$ cells and effects of G-CSF on PKCι activity. A: The expression of PKCι in Trf-R$^+$ and Trf-R$^-$ cells was subjected to Western blot analysis after magnetic cell sorting. B: The G-CSF-dependent PKCι activation of the DMSO-treated HL-60 cells was measured. The x-axis represents the time lapse (min) after the G-CSF stimulation and the y-axis percent of control that was not stimulated by G-CSF. Columns and bars represent the mean ± SD, using data from three separate experiments. Wort: wortmannin (100 nM), GF: GF109207X (10 μM), Gö: Gö6983 (10 μM). Cells were pretreated with each inhibitor and then stimulated by G-CSF for 15 min. C: The PKCι activity in the Trf-R$^+$ and Trf-R$^-$ cells 30 min after the addition of G-CSF. The y-axis represents the percentage of control that was non-stimulated Trf-R$^-$ cells. Columns and bars represent the mean ± SD, using data from three separate experiments.

Effects of G-CSF on PKCι translocation

Muscella et al. (2003) demonstrated that the translocation of PKCζ from the cytosol to the nucleus or membrane is required for c-Fos synthesis induced by angiotensin II in MCF-7 cells. It was also reported that high glucose induced the translocation of PKCι (Chuang et al., 2003). These results suggest that the translocation of aPKC plays an important role in its signaling. To clarify the translocation of PKCι, immuno-histochemical staining (Fig. 3) and biochemical fractionation (Fig. 4) in DMSO-induced HL-60 cells were performed after the addition of G-CSF. In a non-stimulated condition, PKCι in the HL-60 cells treated with DMSO for 2 days (Fig. 3, control) was detected mainly in the nucleus. Analysis of Western blotting (Fig. 4, left parts) and quantification of the bands (Fig. 4, right columns) also revealed that PKCι was localized and observed mainly in the nuclear fraction (Fig. 4A). During the 5–15 min period after the addition of G-CSF, PKCι was found to translocate (Figs. 3 and 4B) into the membrane fraction, after which it re-translocated into the cytosol fraction (Fig. 4C). In the presence of wortmannin, the G-CSF-induced translocation of PKCι into the plasma membrane failed, but PKCι was found to localize in the cytosolic fraction (Figs. 3 and 4B).

Myeloperoxidase is thought to be expressed in stage from promyelocytes to mature neutrophils (Manz et al., 2002). In human cord blood cells (Fig. 3), PKCι in the cells co-stained with anti-myeloperoxidase antibody was also localized in the nucleus after serum depletion (Fig. 3B top parts). Ten minutes after the addition of G-CSF, PKCι was found to translocate into the membrane, and then into the cytosol at 30 min after the addition of G-CSF. In the presence of wortmannin, the G-CSF-induced translocation of PKCι into the plasma membrane failed but PKCι was found to localize in the cytosol. This suggested that the dynamic translocation of PKCι induced by G-CSF is a universal phenomenon in neutrophilic lineage cells. Taken together, these data support the possibility that PI3K plays not only an important role upstream of PKCι but also triggers the translocation from nucleus to membrane upon the addition of G-CSF.

In order to assess the purity of each cellular fraction, antibodies against specific markers were blotted. As specific markers, Histon-H1, Fcγ receptor IIa (CD32), and lactate dehydrogenase (LDH) were used for the nuclear, membrane, and cytosolic fractions, respectively. The purities of the nuclear, membrane, and cytosolic fractions were 82.0, 78.5, and 72.2%, respectively (Fig. 4D).

Effects of siRNA for PKCι on proliferation and differentiation

To determine the role of PKCι in neutrophilic proliferation and differentiation, PKCι was knocked down by siRNA. When the protein level of PKCι was specifically downregulated by siRNA for PKCι (Fig. 5A), G-CSF failed to enhance proliferation of the cells during 5 days' cultivation (Fig. 5B). The effect of siRNA for PKCι on neutrophilic differentiation in terms of fMLP-R expression was also determined. As shown in Figure 5C, fMLP-R expression was promoted by siRNA for PKCι in either the presence (lower part) or absence (upper part) of G-CSF. These data indicate that PKCι positively regulates G-CSF-induced proliferation and negatively regulates the differentiation of DMSO-treated HL-60 cells.

Discussion

We previously reported that PI3K/p70 S6K plays an important role in the regulation of the neutrophilic differentiation and proliferation of HL-60 cells. Akimoto et al. (1998) and Romanelli et al. (1999) reported that p70 S6K is regulated by aPKC and aPKCλ/PKCζ, respectively. At first, we showed that the distribution of PKCζ and PKCι proteins in various human tissues and cells was not similar (Fig. 1A), and that PKCι are more abundantly expressed in proliferating blood cells: Jurkut, K562, U937, and HL-60 cells (Fig. 1B). Moreover, PKCι proteins were also observed in cultured mononuclear cells of cord blood, in which the myeloid progenitors were enriched in the presence or absence of G-CSF (Fig. 1B). The myeloperoxidase-positive cells as neutrophilic lineage cells, a myeloid marker, were also stained with the antibody of PKCι (Fig. 3B). Although PKCζ proteins are barely detected in

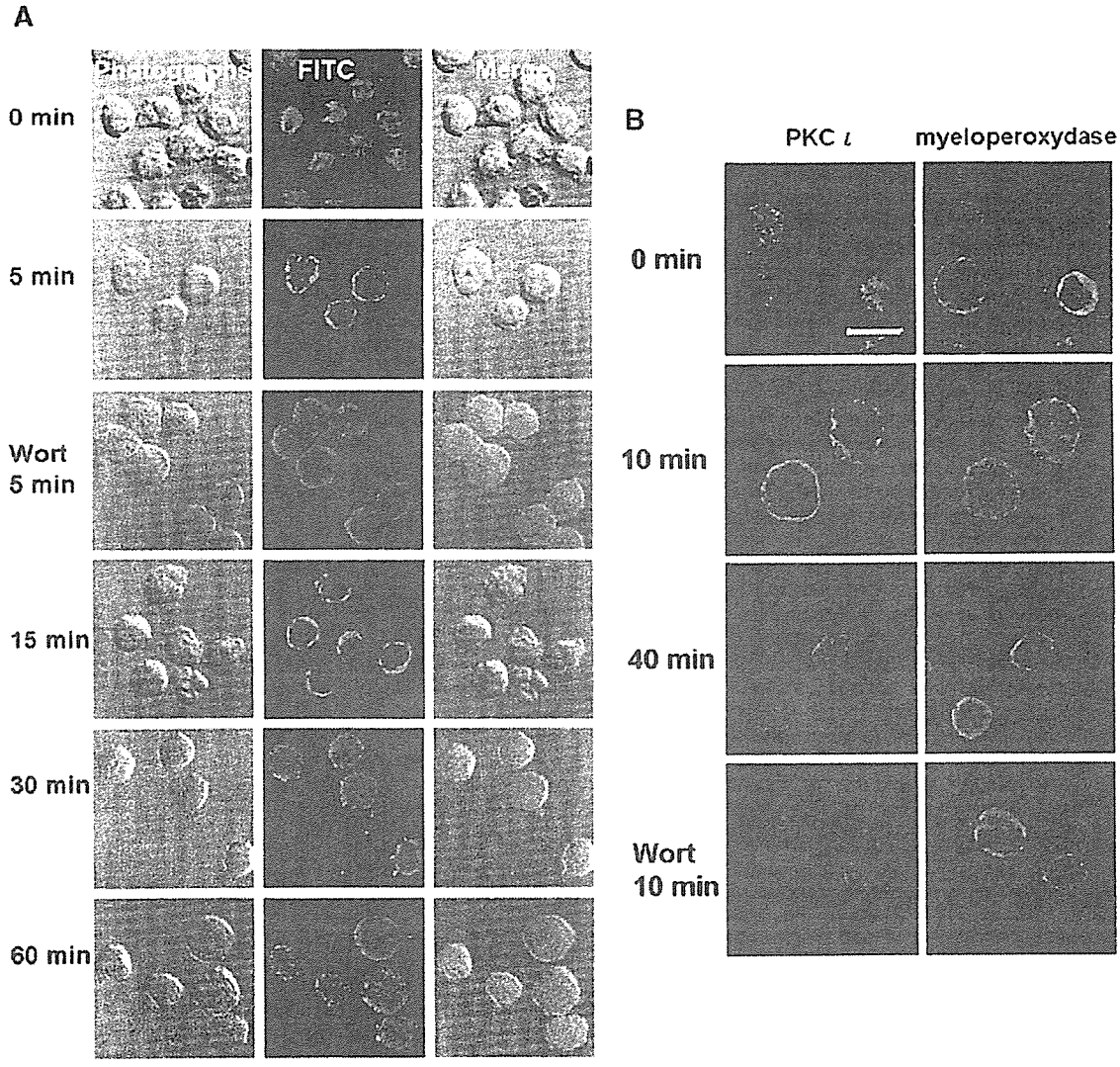

Fig. 3. Translocation of PKCι after the activation of G-CSF. A: 2 days after the addition of DMSO, HL-60 cells stimulated by G-CSF were fixed, incubated with anti-PKCι antibody, and visualized as described above. The photographs can be seen at the left part of the figure, the fluorescent photographs in the middle of the figure, and the merged images at the right. B: G-CSF-stimulated mononuclear cells from cord blood were stained with anti-PKCι antibody (red, left part) and anti-myeloperoxidase antibody (green, right part) after serum depletion. Under no stimulation, PKCι was observed in the nucleus. G-CSF promoted the translocation of PKCι to the membrane within 5–15 min, and then to the cytosol. Wort: wortmannin. White bar: 10 μm.

neutrophilic HL-60 cells, PKCι proteins were markedly expressed in these cells (Fig. 1B). This study showed, for the first time, the stimulation of PKCι activity in G-CSF-treated HL-60 cells (Fig. 2B) at 15–30 min after the addition of G-CSF. Maximum activation from the addition of NGF in PC12 cells was also observed at 15 min (Wooten et al., 2001).

Atypical PKCs are lipid-regulated kinases that need to be localized to the membrane in order to be activated. PKCζ is directly activated by phosphatidylinositol 3,4,5-trisphosphate, a product of PI3K (Nakanishi et al., 1993). We previously reported that the maximum activation of PI3K was observed in HL-60 cells 5 min after the addition of G-CSF (Kanayasu-Toyoda et al., 2002). Most investigators have reported the translocation of aPKC in either muscle cells or adipocytes stimulated by insulin (Andjelkovic et al., 1997; Goransson et al., 1998; Galetic et al., 1999; Standaert et al., 1999; Braiman et al., 2001; Chen et al., 2003; Kanzaki et al., 2004; Sasaoka et al., 2004; Herr et al., 2005). In response to insulin stimulation, aPKCζ/λ is translocated to the plasma membrane (Standaert et al., 1999; Braiman et al., 2001), where aPKCζ/λ is believed to be activated (Galetic et al., 1999; Kanzaki et al., 2004). In the present study, the addition of G-CSF induced PKCι to translocate to the membrane from the nucleus within 5–15 min (Figs. 3 and 4), and this translocation to the plasma membrane accompanied the full activation of PKCι (Fig. 2B). Previously we reported also that the maximum activation of p70 S6K in HL-60 cells was observed from 30 to 60 min after the addition of G-CSF (Kanayasu-Toyoda et al., 1999, 2002), suggesting that there was a time lag between the activation of PI3K and p70 S6K upon the addition of G-CSF in HL-60 cells. In the present study, PKCι was

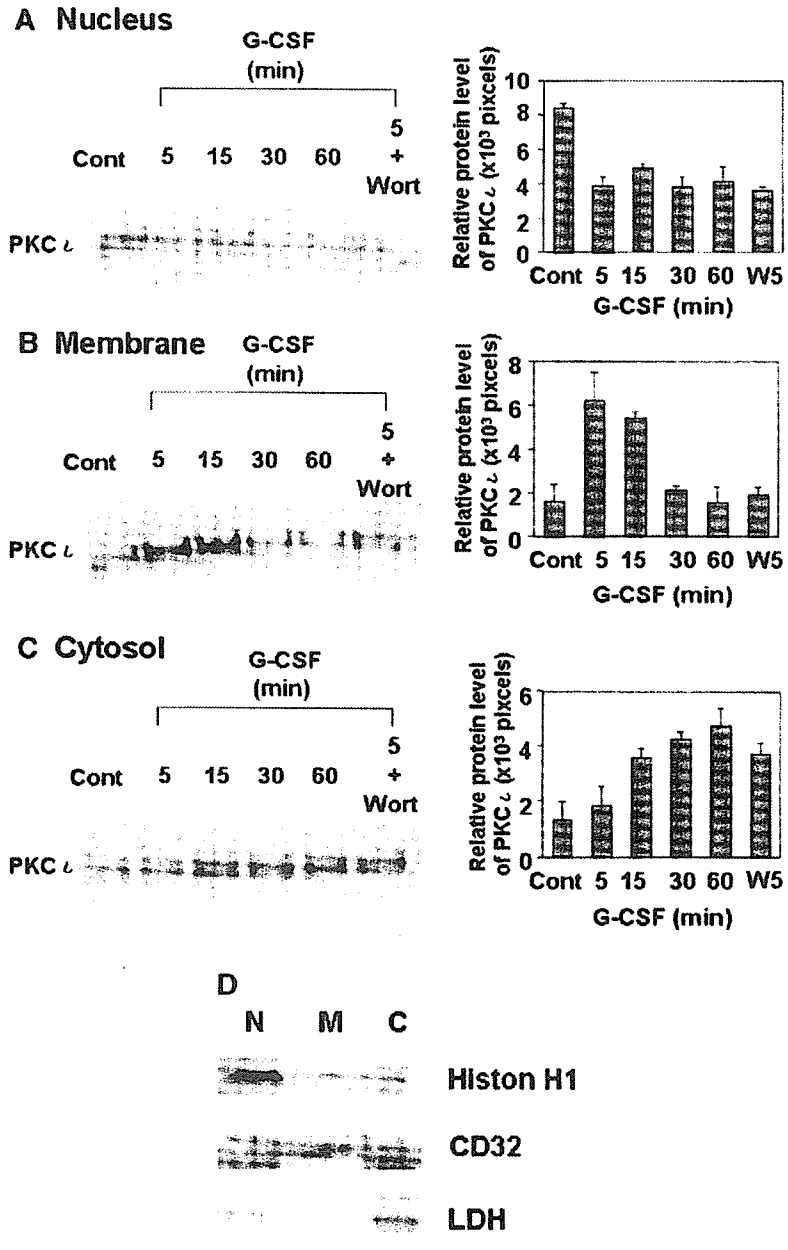

Fig. 4. Translocation of PKCι after activation by G-CSF on biochemical fractionation. The cells were differentiated as described in the Figure 3 legend. After stimulation by G-CSF, the amounts of PKCι proteins in the nucleus (A), plasma membrane (B), and cytosol (C), as fractionated by differential centrifugation, were analyzed by Western blotting (left parts). The right parts show the quantitation of the bands of PKCι proteins. Wort or W: wortmannin. PKCι protein was quantitated using data from three separate experiments. Columns and bars represent the mean ± SD. D: Each cell fraction was immunoblotted with antibodies of specific marker. Histon-H1, Fcγ receptor IIa (CD32), and lactate dehydrogenase (LDH) are specific markers for nuclear (N), membrane (M), and cytosolic (C) fractions, respectively.

found to re-translocate from the plasma membrane to the cytosol (Figs. 3 and 4C). In the presence of wortmannin, an inhibitor of PI3K, PKCι failed to translocate into the plasma membrane, but instead translocated to cytosol directly from the nucleus upon the addition of G-CSF (Figs. 3 and 4B). PKCι translocation was also observed in myeloperoxidase-positive cells derived from human cord blood (Fig. 3B), indicating that G-CSF-induced dynamic translocation of PKCι occurred in not only a limited cell line but also neutrophilic lineage cells. These data suggest that PI3K plays an important role in the activation and translocation of PKCι during the G-CSF-induced activation of myeloid cells. Furthermore, the translocation to the plasma membrane in response to G-CSF is wortmannin sensitive, but the translocation from the nucleus upon G-CSF stimulation is not affected by wortmannin, suggesting that the initial signal of G-CSF-induced PKCι translocation from the nucleus may be

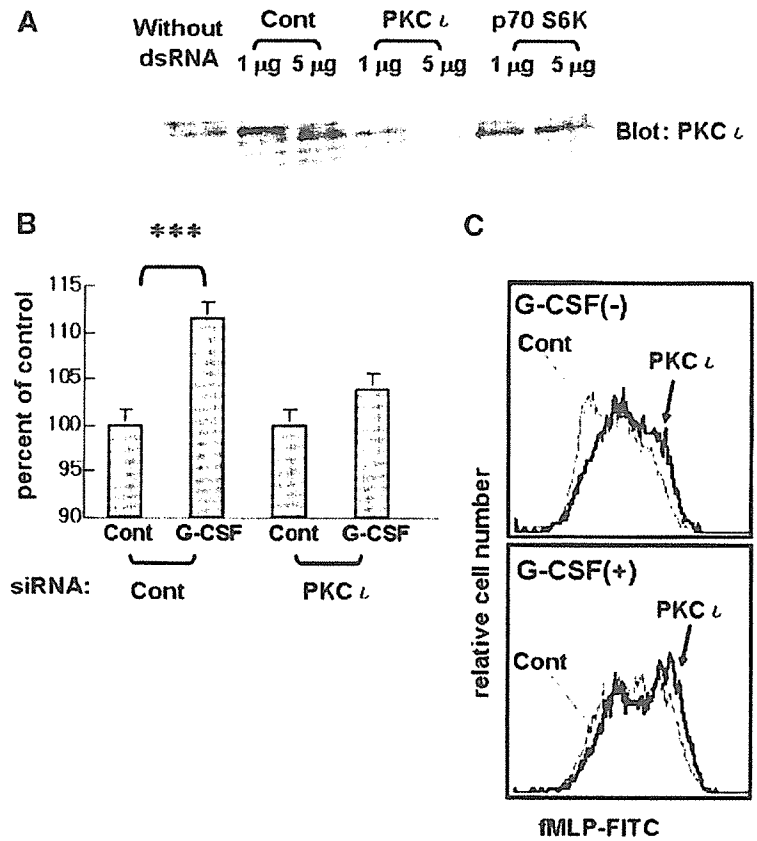

Fig. 5. Effects of siRNA of PKCι on proliferation, differentiation, and phosphorylation at various sites of p70 S6K. A: Forty-eight hours after transfection with siRNA of PKCι or p70 S6K, protein levels of PKCι were compared. B: Proliferation of the cells transfected with siRNA of PKCι or control (Cont) was measured 5 days after the addition of G-CSF. Columns and bars represent the mean ± SD of triplicate wells (*$P < 0.001$). C: fMLP-R expression was analyzed by flow cytometry 5 days after the addition of G-CSF. The gray arrow indicates cells transfected with the control sequence of double-stranded RNA (Cont, gray lines), and the black arrow the cells transfected with siRNA for PKCι (black lines) in the presence (lower part) or absence (upper part) of G-CSF.**

PI3K-independent, but association of PKCι with the plasma membrane could be mediated through a PI3K-dependent signal. Cord blood is an important material of blood transplantation for leukemia (Bradstock et al., 2006; Ooi, 2006; Yamada et al., 2006) or for congenital neutropenia (Mino et al., 2004; Nakazawa et al., 2004) because it contains many hematopoietic stem cells such as CD34-positive cells or CD133-positive cells, and also contains immature granulocytes. The neutrophilic differentiation and proliferation are necessary processes after transplantation.

Formyl-Met-Leu-Phe peptide evokes the migration, superoxide production, and phagocytosis of neutrophils through fMLP-R, a suitable marker for neutrophilic differentiation. In this study, the reduction of PKCι by siRNA inhibited G-CSF-induced proliferation (Fig. 5B) and promoted neutrophilic differentiation (Fig. 5C) in terms of fMLP-R expression. These data, however, suggest that PKCι promoted G-CSF-induced proliferation and blocked differentiation at the same time.

The substrates of aPKC have recently been reported: namely, the cytoskeletal protein Lethal giant larvae (Lgl) was phosphorylated by Drosophila aPKC (Betschinger et al., 2003) and glyceraldehydes-3-phosphate dehydrogenase (GAPDH) was phosphorylated by PKCι (Tisdale, 2002) directly in both cases. While the direct phosphorylation of p70 S6K by aPKC was not observed (Akimoto et al., 1998; Romanelli et al., 1999), the enzyme activity of p70 S6K was markedly enhanced by co-transfection with aPKC and PDK-1, the latter of which is recruited to the membrane due to the binding of phosphatidylinositol-3,4,5-trisphosphate to its PH domain (Anderson et al., 1998). The addition of G-CSF induced PKCι to increase phosphorylation at Thr-389, which is the site most closely related to enzyme activity among the multi-phosphorylation sites of p70 S6K (Weng et al., 1998). However, the mammalian target of rapamycin (mTOR), an upstream regulator, also phosphorylates Thr-389 of p70 S6K and markedly stimulates p70 S6K activity under coexistence with PDK-1 (Isotani et al., 1999). We could not rule out the possibility that other PKC isoforms can contribute to the activation of p70 S6K. We postulated that in G-CSF-stimulated HL-60 cells, PKCι contributes to p70 S6K activation as an upstream regulator.

Atypical PKC isoforms are reported to play an important role in the activation of IκB kinase β (Lallena et al., 1999). In PKCζ-deficient mice, impaired signaling through the B-cell receptor resulted in the inhibition of cell proliferation and survival while also causing defects in the activation of ERK and the transcription of NF-κB-dependent genes (Martin et al., 2002). Moreover, Lafuente et al. (2003) demonstrated that the loss of Par-4, that is, the genetic inactivation of the aPKC inhibitor, led to an increased proliferative response of

peripheral T cells when challenged through the T-cell receptor. However, it has been reported that PKCλ-deficient mice have a lethal phenotype at the early embryonic stage (Soloff et al., 2004). Based on the present results and those of previous reports (Kanayasu-Toyoda et al., 1999, 2002), we postulate that PKCι plays an important role in regulating G-CSF-induced proliferation in neutrophilic lineage cells.

Acknowledgments

We thank the Metro Tokyo Red Cross Cord Blood Bank (Tokyo, Japan) for their kind cooperation. This work was supported in part by a grand-in-aid for health and labor science research (H17-SAISEI-021) from the Japanese Ministry of Health, Labor and Welfare, and in part by a grand-in-aid for Research on Health Sciences focusing on Drug Innovation from the Japan Health Sciences Foundation.

Literature Cited

Akimoto K, Nakaya M, Yamanaka T, Tanaka J, Matsuda S, Weng QP, Avruch J, Ohno S. 1998. Atypical protein kinase Clambda binds and regulates p70 S6 kinase. Biochem J 335:417–424.

Anderson KE, Coadwell J, Stephens LR, Hawkins PT. 1998. Translocation of PDK-1 to the plasma membrane is important in allowing PDK-1 to activate protein kinase B. Curr Biol 8:684–691.

Andjelkovic M, Alessi DR, Meier R, Fernandez A, Lamb NJ, Frech M, Cron P, Cohen P, Lucocq JM, Hemmings BA. 1997. Role of translocation in the activation and function of protein kinase B. J Biol Chem 272:31515–31524.

Betschinger J, Mechtler K, Knoblich JA. 2003. The Par complex directs asymmetric cell division by phosphorylating the cytoskeletal protein Lgl. Nature 422:326–330.

Bradstock KF, Hertzberg MS, Kerridge IH, Svennilson J, McGurgan M, Huang G, Antonenas V, Gottlieb DJ. 2006. Unrelated umbilical cord blood transplantation for adults with haematological malignancies: Results from a single Australian centre. Intern Med J 36:355–361.

Braiman L, Alt A, Kuroki T, Ohba M, Bak A, Tennenbaum T, Sampson SR. 2001. Activation of protein kinase C zeta induces serine phosphorylation of VAMP2 in the GLUT4 compartment and increases glucose transport in skeletal muscle. Mol Cell Biol 21:7852–7861.

Chen X, Al-Hasani H, Olausson T, Wenthzel AM, Smith U, Cushman SW. 2003. Activity, phosphorylation state and subcellular distribution of GLUT4-targeted Akt2 in rat adipose cells. J Cell Sci 116:3511–3518

Chuang LY, Goh JY, Liu SF, Hung MY, Liao TN, Chiang TA, Huang JS, Huang YL, Lin CF, Yang YL. 2003. Regulation of type II transforming-growth-factor-beta receptors by protein kinase C iota. Biochem J 375:385–393.

Chung J, Grammer TC, Lemon KP, Kazlauskas A, Blenis J. 1994. PDGF- and insulin-dependent p70 S6K activation mediated by phosphatidylinositol-3-OH kinase. Nature 370:71–75.

Debili N, Robin C, Schiavon V, Letestu R, Pflumio F, Mitjavila-Garcia MT, Coulombel L, Vainchenker W. 2001. Different expression of CD41 on human lymphoid and myeloid progenitors from adults and neonates. Blood 97:2023–2030.

Fritsch G, Buchinger P, Printz D, Fink FM, Mann G, Peters C, Wagner T, Adler A, Gadner H. 1993. Rapid discrimination of early CD34+ myeloid progenitors using CD45 RA analysis. Blood 81:2301–2309.

Galetic I, Andjelkovic M, Meier R, Brodbeck D, Park J, Hemmings BA. 1999. Mechanism of protein kinase B activation by insulin/insulin-like growth factor-1 revealed by specific inhibitors of phosphoinositide 3-kinase—Significance for diabetes and cancer. Pharmacol Ther 82:409–425.

Goransson O, Wijkander J, Manganiello V, Degerman E. 1998. Insulin-induced translocation of protein kinase B to the plasma membrane in rat adipocytes. Biochem Biophys Res Commun 246:249–254.

Hao QL, Zhu J, Price MA, Payne KJ, Barsky LW, Crooks GM. 2001. Identification of a novel, human multilymphoid progenitor in cord blood. Blood 97:3683–3690.

Herr HJ, Bernard JR, Reeder DW, Rivas DA, Limon JJ, Yaspelkis BB3rd. 2005. Insulin-stimulated plasma membrane association and activation of Akt2, aPKC zeta and aPKC lambda in high fat fed rodent skeletal muscle. J Physiol 565:627–636.

Huang S, Chen Z, Yu JF, Young D, Bashey A, Ho AD, Law P. 1999. Correlation between IL-3 receptor expression and growth potential of human CD34+ hematopoietic cells from different tissues. Stem Cells 17:265–272.

Isotani S, Hara K, Tokunaga C, Inoue H, Avruch J, Yonezawa K. 1999. Immunopurified mammalian target of rapamycin phosphorylates and activates p70 S6 kinase alpha in vitro. J Biol Chem 274:34493–34498.

Kanayasu-Toyoda T, Yamaguchi T, Uchida E, Hayakawa T. 1999. Commitment of neutrophilic differentiation and proliferation of HL-60 cells coincides with expression of transferrin receptor. Effect of granulocyte colony stimulating factor on differentiation and proliferation. J Biol Chem 274:25471–25480.

Kanayasu-Toyoda T, Yamaguchi T, Oshizawa T, Kogi M, Uchida E, Hayakawa T. 2002. Role of the p70 S6 kinase cascade in neutrophilic differentiation and proliferation of HL-60 cells—a study of transferrin receptor-positive and -negative cells obtained from dimethyl sulfoxide- or retinoic acid-treated HL-60 cells. Arch Biochem Biophys 405:21–31.

Kanayasu-Toyoda T, Yamaguchi T, Oshizawa T, Uchida E, Hayakawa T. 2003. The role of c-Myc on granulocyte colony-stimulating factor-dependent neutrophilic proliferation and differentiation of HL-60 cells. Biochem Pharmacol 66:133–140.

Kanzaki M, Mora S, Hwang JB, Saltiel AR, Pessin JE. 2004. Atypical protein kinase C (PKCzeta/lambda) is a convergent downstream target of the insulin-stimulated phosphatidylinositol 3-kinase and TC10 signaling pathways. J Cell Biol 164:279–290.

Lafuente MJ, Martin P, Garcia-Cao I, Diaz-Meco MT, Serrano M, Moscat J. 2003. Regulation of mature T lymphocyte proliferation and differentiation by Par-4. Embo J 22:4689–4698.

Lallena MJ, Diaz-Meco MT, Bren G, Paya CV, Moscat J. 1999. Activation of IkappaB kinase beta by protein kinase C isoforms. Mol Cell Biol 19:2180–2188.

Liu WS, Heckman CA. 1998. The sevenfold way of PKC regulation. Cell Signal 10:529–542.

Manz MG, Miyamoto T, Akashi K, Weissman IL. 2002. Prospective isolation of human clonogenic common myeloid progenitors. Proc Natl Acad Sci USA 99:11872–11877.

Martin P, Duran A, Minguet S, Gaspar ML, Diaz-Meco MT, Rennert P, Leitges M, Moscat J. 2002. Role of zeta PKC in B-cell signaling and function. Embo J 21:4049–4057.

Mino E, Kobayashi R, Yoshida M, Suzuki Y, Yamada M, Kobayashi K. 2004. Umbilical cord blood stem cell transplantation from unrelated HLA-matched donor in an infant with severe congenital neutropenia. Bone Marrow Transplant 33:969–971.

Muscella A, Greco S, Elia MG, Storelli C, Marsigliante S. 2003. PKC-zeta is required for angiotensin II-induced activation of ERK and synthesis of C-FOS in MCF-7 cells. J Cell Physiol 197:61–68.

Nakanishi H, Brewer KA, Exton JH. 1993. Activation of the zeta isozyme of protein kinase C by phosphatidylinositol 3,4,5-trisphosphate. J Biol Chem 268:13–16.

Nakazawa Y, Sakashita K, Kinoshita M, Saida K, Shigemura T, Yanagisawa R, Shikama N, Kamijo T, Koike K. 2004. Successful unrelated cord blood transplantation using a reduced-intensity conditioning regimen in a 6-month-old infant with congenital neutropenia complicated by severe pneumonia. Int J Hematol 80:287–290.

Nguyen BT, Dessauer CW, 2005. Relaxin stimulates protein kinase C zeta translocation: Requirement for cyclic adenosine 3',5'-monophosphate production. Mol Endocrinol 19:1012–1023.

Oo J. 2006. The efficacy of unrelated cord blood transplantation for adult myelodysplastic syndrome. Leuk Lymphoma 47:599–602.

Rappold I, Ziegler BL, Kohler I, Marchetto S, Rosnet O, Birnbaum D, Simmons PJ, Zannettino AC, Hill B, Neu S, Knapp W, Alitalo R, Alitalo K, Ullrich A, Kanz L, Buhring HJ. 1997. Functional and phenotypic characterization of cord blood and bone marrow subsets expressing FLT3 (CD135) receptor tyrosine kinase. Blood 90:111–125.

Romanelli A, Martin KA, Toker A, Blenis J. 1999. p70 S6 kinase is regulated by protein kinase Czeta and participates in a phosphoinositide 3-kinase-regulated signalling complex. Mol Cell Biol 19:2921–2928.

Sasaoka T, Wada T, Fukui K, Murakami S, Ishihara H, Suzuki R, Tobe K, Kadowaki T, Kobayashi M. 2004. SH2-containing inositol phosphatase 2 predominantly regulates Akt2, and not Akt1, phosphorylation at the plasma membrane in response to insulin in 3T3-L1 adipocytes. J Biol Chem 279:14835–14843.

Selbie LA, Schmitz-Peiffer C, Sheng Y, Biden TJ. 1993. Molecular cloning and characterization of PKC iota, an atypical isoform of protein kinase C derived from insulin-secreting cells. J Biol Chem 268:24296–24302.

Soloff RS, Katayama C, Lin MY, Feramisco JR, Hedrick SM. 2004. Targeted deletion of protein kinase C lambda reveals a distribution of functions between the two atypical protein kinase C isoforms. J Immunol 173:3250–3260.

Standaert ML, Bandyopadhyay G, Perez L, Price D, Galloway L, Poklepovic A, Sajan MP, Cenni V, Sirri A, Moscat J, Toker A, Farese RV. 1999. Insulin activates protein kinases C-zeta and C-lambda by an autophosphorylation-dependent mechanism and stimulates their translocation to GLUT4 vesicles and other membrane fractions in rat adipocytes. J Biol Chem 274:25308–25316.

Tenen DG, Hromas R, Licht JD, Zhang DE. 1997. Transcription factors, normal myeloid development, and leukemia. Blood 90:489–519.

Tisdale EJ. 2002. Glyceraldehyde-3-phosphate dehydrogenase is phosphorylated by protein kinase Ciota/lambda and plays a role in microtubule dynamics in the early secretory pathway. J Biol Chem 277:3334–3341.

Ward AC, Loeb DM, Soede-Bobok AA, Touw IP, Friedman AD. 2000. Regulation of granulopoiesis by transcription factors and cytokine signals. Leukemia 14:973–990.

Weng QP, Kozlowski M, Belham C, Zhang A, Comb MJ, Avruch J. 1998. Regulation of the p70 S6 kinase by phosphorylation in vivo. Analysis using site-specific anti-phosphopeptide antibodies. J Biol Chem 273:16621–16629.

Wooten MW, Vandenplas ML, Seibenhener ML, Geetha T, Diaz-Meco MT. 2001. Nerve growth factor stimulates multisite tyrosine phosphorylation and activation of the atypical protein kinase C's via a src kinase pathway. Mol Cell Biol 21:8414–8427.

Yamada K, Mizusawa M, Harima A, Kajiwara K, Hamaki T, Hoshi K, Kozai Y, Kodo H. 2006. Induction of remission of relapsed acute myeloid leukemia after unrelated donor cord blood transplantation by concomitant low-dose cytarabine and calcitriol in adults. Eur J Haematol 77:345–348.

Yamaguchi T, Mukasa T, Uchida E, Kanayasu-Toyoda T, Hayakawa T. 1999. The role of STAT3 in granulocyte colony-stimulating factor-induced enhancement of neutrophilic differentiation of Me2SO-treated HL-60 cells. GM-CSF inhibits the nuclear translocation of tyrosine-phosphorylated STAT3. J Biol Chem 274:15575–15581.

Genes and Environment, Vol. 28, No. 2 pp. 68-73 (2006)

Regular article

Microcystin-LR is not Mutagenic *in vivo* in the λ/*lacZ* Transgenic Mouse (Muta™Mouse)

Li Zhan[1,2], Masamitsu Honma[2], Li Wang[1], Makoto Hayashi[2], De-Sheng Wu[4], Li-Shi Zhang[4], Palanichamy Rajaguru[3,5] and Takayoshi Suzuki[2,3,6]

[1]National Chengdu Center for Safety Evaluation of Traditional Chinese Medicine, West China Hospital, Sichuan University, Chengdu, China
[2]Division of Genetics and Mutagenesis, [3]Division of Cellular and Gene Therapy Products, National Institute of Health Sciences, Tokyo, Japan
[4]West China School of Public Health, Sichuan University, Chengdu, China
[5]Department of Biotechnology, School of Engineering and Technology, Bharathidasan University, Tiruchirappalli, India

(Received April 2, 2006; Accepted April 18, 2006)

The water pollution of toxic cyanobacteria (blue-green algae) is causing a serious public health problem in many parts of the world. Microcystin-LR (MCLR) is a potent cyclic heptapeptidic hepatotoxin produced by the cyanobacterium *Microcystis aeruginosa*. MCLR presents acute and chronic hazards to human health and has been linked to primary liver cancer in humans chronically exposed to this peptide toxin through drinking water. To assess the *in vivo* mutagenecity of MCLR, the λ/*lacZ* transgenic mice (Muta™Mouse) were treated with MCLR (1 mg/kg per week x 4) and examined for mutant frequencies (MFs) in the *lacZ* and *cII* genes of liver and lungs. Micronucleus induction in peripheral blood cells was also assessed. Co-mutagenic effect of MCLR was studied in combination with *N*-nitrosodiethylamine (DEN). MCLR did not increase either MFs of the target genes in liver and lungs or micronucleus frequency in the peripheral blood cells of the λ/*lacZ* transgenic mouse. While DEN treatment increased MFs significantly, the co-administration of MCLR did not potentiate its mutagenicity. We conclude that pure MCLR has no *in vivo* mutagenicity as it failed to induce gene mutation and micronucleus in transgenic mouse. Its tumor promoting effect is independent of its interaction to DNA.

Key words: Microcystin-LR, *N*-nitrosodiethylamine, *lacZ*, *cII*, Muta™Mouse

Introduction

The water pollution of toxic cyanobacterial bloom (blue-green algae) is an increasing problem worldwide and worsens with eutrophication of drinking- and recreational- water reservoirs due to industrialization (1,2). Cyanobacteria produce lethal toxins, and often associated to death of livestock and cases of human illness caused by drinking water contaminated by these toxins, which have drawn the attention of the World Health Organization (WHO) (3). Microcystins are the most common group of cyanobacterial toxins comprised of over 60 structurally related cyclic heptapeptides (4) with potent hepatotoxicity and tumor promotion ability (5,6). Among them, Microcystin-LR (MCLR) is the most frequent secondary metabolite produced by *Microcystis aeruginosa* (2,7). MCLR presents acute and chronic hazards to human health (8,9). Although human illnesses attributed to microcystins include gastroenteritis and allergic/irritation reactions, the primary target of the toxin is the liver (10-14). It has been suspected to be involved with promotion of primary liver cancer in humans chronically exposed to doses of these peptide toxins through drinking water (15,16).

Algal toxins were reported to cause chromosomal breakages in human lymphocytes *in vitro* (17). Genotoxicity of cynobacterial extract has been demonstrated by SOS chromotest with *Escherichia coli* PQ37 and the comet assay with human lymphocytes (18) and in four strains of *Salmonella typhimurium* (TA97, TA98, TA100 and TA102) in Ames test with or without S9 mix (19). In the same study, however, pure MCLR did not show any mutagenicity in all these strains. MCLR was reported to damage the mitotic spindle apparatus and thus induces polyploidy and apoptosis and necrosis in Chinese hamster ovary (CHO-K1) cells (20), and to induce gene mutation with base substitution in human RSa cells (21). Recently we have demonstrated mutagenic and clastogenic activities of MCLR in human lymphoblastoid cells (TK6) after 24 h treatment *in vitro*

[6]Correspondence to: Takayoshi Suzuki, Division of Cellular and Gene Therapy Products, National Institute of Health Sciences, 1-18-1 Kamiyoga, Setagaya-ku, Tokyo 158-8501, Japan. Tel: +81-3-3700-1926, Fax: +81-3-3700-1926, E-mail suzuki@nihs.go.jp

(22). Because MCLR induced mainly LOH type mutations rather than point mutations, mutagenicity of MCLR might be exerted by a clastogenic mechanism. Nevertheless, *in vivo* genotoxicity of this cyanotoxin is less convincing and relatively undescribed. Therefore, the present study was conducted to evaluate the *in vivo* mutagenicity of MCLR using transgenic (TG) mouse mutation assay. TG system has been shown to be useful for studying chemical mutagenesis and clastogenesis *in vivo* (23–25). This is largely attributed to its ability to detect tissue-specific gene mutations. TG assay also permits analysis of mutation at the molecular level and allows examination of the relation between mutagenesis and carcinogeneis *in vivo* in detail (25). Since MCLR has been found to promote tumor initiated with *N*-nitrosodiethylamine (DEN) in rats (5), the co-mutagenic (potentiation) effects of MCLR in combination with DEN was also studied.

Materials and Methods

Chemicals: MCLR and DEN were purchased from Wako Pure Chemical Industries, Ltd. (Osaka, Japan). MCLR was dissolved in saline immediately before use. Phenyl-β-D-galactoside (P-gal) was purchased from Sigma.

Treatment of Muta™Mice: Male Muta™Mice (5-6-week old, ca. 25 g body weight) supplied by Covance Research Products (PA, USA) were acclimatized for 1 week before use. The animals were divided into 4 groups of 5 mice each and administered with weekly doses of either vehicle (saline), MCLR (1 mg/kg, 1/10 of LD_{50} in mice), DEN (25 mg/kg, 1/4 of LD_{50} in mice) or DEN + MCLR (25 mg/kg and 1 mg/kg, respectively) for 4 weeks. Saline and MCLR were administered intragastrically while DEN was intraperitonealy injected. No apparent sign of toxicity was observed in any mice.

Micronucleus assay in peripheral blood cells: Forty eight hours after the first treatment, 5 μL of peripheral blood was collected from the tail vein without anti-coagulant. The blood thus collected from each animal was placed on an acridine orange-coated glass slide, covered with a cover slip, and supravitally stained (26). Type I, II, and III reticulocytes (RETs) with red fluorescent reticulum in the cytoplasm were scored under a fluorescent microscope. One thousand RETs were examined per animal within a few days after the slide preparation. The number of RETs with micronucleus (MNRETs) was recorded.

Mutation assay: 1) Tissue collection: Mice were killed by cervical dislocation 7 days after the last treatment. Liver and lungs were removed, immediately frozen in liquid nitrogen, and stored at −80°C until DNA extraction. MFs of *lacZ/cII* transgenes derived from liver and lungs were determined as described previously (27–29). DNA sequencing of mutants isolated from the control and MCLR treated animals were carried out as described below.

2) Sequence analysis of *cII* gene: The *cII*-mutant plaques were transferred into a microtube containing 50 μL SM buffer and 5 μL chloroform. The λ phage *cII* region was amplified directly from mutant plaque solution by Taq DNA polymerase (Takara Shuzo, Tokyo, Japan) with primers P1, 5′-AAAAAGGGCAT-CAAATTAAACC-3′; and P2, 5′-CCGAAGTTGAG-TATTTTTG- CTGT-3′. Amplification was done by the Minicycler PTC-150-25 (MJ Research, Inc., MA, USA) under the following thermal cycling: 95°C 5 min→ (95°C 20 s, 53°C 30 s, 72°C 40 s) × 30 cycles→72°C 10 min. Amplification of 446 bp PCR product was checked by 2100 Bioanalyzer using lab DNA chips (Agilent Technologies, USA) and purified with a microspin column (Amersham Pharmacia, Tokyo, Japan) before being used for a sequencing reaction with the Ampli Taq cycle sequencing kit (PE Biosystems, Tokyo, Japan). The sequencing reaction was performed by Minicycler PTC-150-25 with 25 cycles of denaturing at 96°C for 10 s, annealing at 50°C for 5 s, and extension at 60°C for 4 min, with the primer P1. The reaction product was purified by ethanol precipitation and analyzed by the ABI PRISM® 310 Genetics Analyzer (PE Biosystems, Tokyo, Japan).

3) Statistical analysis: The results of the different treatment groups were compared using Students' *t*-test. Significance was indicated by P values <0.05.

Results

Micronucleus induction in peripheral blood: Results of the micronucleus test 48 h after the first administration of chemicals in the Muta™Mice is shown in Fig. 1. The mean frequency of MNRETs did not increase significantly ($P>0.05$) in any of the treatment group in comparison with that of the control group.

Mutant frequency of *lacZ* and *cII* genes: The mutant frequencies (MFs) observed in the DNA preparations extracted from the liver and lung tissues 7 days after the last treatment are shown in Table 1. In MCLR-treated mice, the MFs of *lacZ* and *cII* genes in liver were not different significantly ($P>0.05$) from that of the background levels. Although a slight increase was observed in the lungs, it was not statistically significant ($P>0.05$). DEN treatment significantly ($P<0.05$) increased MFs of both the target genes in both liver and lungs (for *lacZ* gene 6.1 fold and 3.7 fold respectively and for *cII* gene 11.0 fold and 4.6 fold, respectively). We did not observe significant difference in MFs between DEN-treated and DEN + MCLR co-treated animals.

***cII* mutation spectrum:** Thirty four MCLR-in-